Afd. Historische Geografie

Integrated use of hydrological modelling and remote sensing in the Province of Drenthe

# Integrated use of hydrological modelling and remote sensing in the Province of Drenthe

## Possibilities and restrictions

Sandra M.L. Verheijden

Report 61

DLO Winand Staring Centre, Wageningen (The Netherlands), 1992

ABSTRACT

Verheijden, S.M.L., 1992. *Integrated use of hydrological modelling and remote sensing in the Province of Drenthe; possibilities and restrictions.* Wageningen (The Netherlands), DLO Winand Staring Centre. Report 61. 81 pp; 20 Figs; 19 Tables; 27 Refs.

For the eastern part of the Province of Drenthe an investigation of the possibilities of an integrated use of hydrological modelling and remote sensing was performed. A comparison was made between relative crop transpiration values according to the remote sensing approach and as simulated with the model SWACROP. Great deviations occurred between the relative crop transpiration values calculated with both methods. In contradiction with the expectations a more detailed SWACROP input did not improve the correspondence of SWACROP and remote sensing results. It is expected that the deviations are mainly caused by differences in temporal and spatial scale. Moreover the importance of visual interpretation of remote sensing images has proven to be a valuable tool in the validation of a seepage/infiltration map.

Keywords: relative crop transpiration, SWACROP, visual interpretation, seepage/infiltration.

ISSN 0927-4537



Project 10034 [050Cis/10.92]

CONTENTS


| | | page |
|---|---|---|
| PREFACE | | 9 |
| SUMMARY | | 11 |
| 1 | INTRODUCTION | 15 |
| 2 | SWACROP | 16 |
| 2.1 | Basic flow equation | 16 |
| 2.2 | Boundary conditions at the top of the system | 17 |
| 2.2.1 | Potential evapotranspiration | 17 |
| 2.2.2 | Potential soil evaporation | 17 |
| 2.2.3 | Potential crop transpiration | 19 |
| 2.2.4 | Actual soil evaporation | 19 |
| 2.2.5 | Actual crop transpiration | 20 |
| 2.2.6 | Relative crop transpiration | 21 |
| 2.3 | Boundary conditions at the bottom of the system | 21 |
| 2.4 | Input data | 21 |
| 2.4.1 | Meteorological data | 22 |
| 2.4.2 | Ground water levels | 22 |
| 2.4.3 | Soil and hydrology | 22 |
| 2.4.4 | Crop | 22 |
| 2.4.5 | Additional input data | 26 |
| 3 | REMOTE SENSING | 29 |
| 3.1 | Data | 29 |
| 3.2 | False colour photographs | 29 |
| 3.3 | Airborne Multispectral Scanning (MSS) and Infrared Line Scanning (IRLS) | 30 |
| 3.4 | Crop type classification | 31 |
| 3.5 | Evapotranspiration mapping | 32 |
| 4 | COMPARISON OF REMOTE SENSING AND SWACROP RELATIVE CROP TRANSPIRATION VALUES | 37 |
| 4.1 | Description of the study area | 37 |
| 4.2 | Large scale comparison of remote sensing and SWACROP relative crop transpiration values | 37 |
| 4.3 | Detailed comparison of SWACROP and remote sensing relative crop transpiration values | 40 |
| 4.4 | Results and discussion | 40 |
| 4.4.1 | Variation in crop transpiration values | 40 |
| 4.4.2 | Comparison on individual locations | 42 |

page

5 HYDROLOGICAL MAPPING EXPERIMENT APPLYING REMOTE SENSING 47
5.1 Composition of the seepage infiltration map Drenthe (1 : 100 000) 47
5.2 Use of remote sensing images 48
5.3 Results and discussion 49

6 CONCLUSIONS AND DISCUSSION 53

REFERENCES 55

ANNEX
1 Crop type classification and soil map for map numbers 12 Oost and 17 Oost 59
2 Global description of the main soil groups on map numbers 12 Oost and 17 Oost 61
3 Overview of main soil groups, thickness of the layers they consist of and the effective root zone for potatoes, beets grass, cereals and maize 63
4 Description of a SWACROP input file 67
5 Description of ground water table classes 71
6 Overview of all simulation results 73
7 Part of the seepage infiltration map Drenthe (1989) 75
8 Seepage infiltration map for the Northern part of map number 12 Oost 77
9 MODFLOW output values combined with an overlay of the seepage infiltration map 79
10 Soil map combined with an overlay of the seepage infiltration map 81

FIGURES
1 General shape of the dimensionless sink term variable $\alpha$ 20
2 Fraction of soil covered for a standard growing season for potatoes 24
3 Fraction of soil covered for a standard growing season for cereals, beets and maize 24
4 Shape of the reduction factor $\alpha$ in the Sink term as a function of h 26
5 Scheme of the soil system and the calculated fluxes 27
6 Multispectral scanner system operation 31
7 Relative crop transpiration map for map numbers 12 Oost and 17 Oost on June 20 and August 23, 1989 35
8 Situation of map numbers 12 Oost and 17 Oost in the Province of Drenthe 39
9 Relative crop transpiration distribution according to remote sensing and SWACROP simulation results on June 20 and August 23 for map numbers 12 Oost and 17 Oost 41

page

10 Relative crop transpiration distribution according to remote sensing and SWACROP simulation results for beets, grass and maize on August 23 (map numbers 12 Oost and 17 Oost) 41
11 Remote sensing relative crop transpiration values against SWACROP relative crop transpiration values for all observation wells 42
12 Examples of regular and irregular transpiring fields 43
13 Overlay of the seepage/infiltration map on a combined relative crop transpiration image 51
14 Proposal for some modifications in the seepage/infiltration map Drenthe 51
15 Crop type classification for the growing season of 1989 for map number 12 Oost and 17 Oost 59
16 Generalized soil map for map numbers 12 Oost and 17 Oost 59
17 Part of the seepage/infiltration map Drenthe (1989) 75
18 Seepage/infiltration map for the northern part of map number 12 Oost 77
19 Flux from first to second model layer as calculated with the model MODFLOW combined with an overlay of the seepage/infiltration map (northern part of map number 12 Oost) 79
20 Soil-water table class map with an overlay of the seepage/infiltration map for the northern part of map number 12 Oost 81

TABLES

1 Simulated crops with their sowing and harvesting days (Julian day numbers) 23
2 Values for the crop dependent constants a, b, and c used in the Leaf Area Index function 23
3 The crop factors per decade and the corresponding input days 25
4 Growth rate of the rooting system during the growing season and the maximum rooting depth for potatoes, maize, beets, cereals and grass 25
5 Pressure heads that describe the reduction factor $\alpha$ for potatoes, maize, beets, cereals and grass 26
6 Data and applications in the Remote Sensing Project Drenthe 29
7 Condition of different crops on the flight days 30
8 Available scanner data, the spectral bands and the ground resolution 30
9 Values of regression coefficients for different crops at standard heights 34
10 Mean difference between remote sensing and SWACROP relative crop transpiration values for the different simulated crops and soil types 45
11 Number of measurements for each combination of soil type and crop 45
12 Materials used to compose the seepage infiltration map Drenthe (1 : 100 000) 47

page

13 Main soil groups, thickness of the layers they consist of and the effective root zone for potatoes and beets 63
14 Main soil groups, thickness of the layers they consist of and the effective root zone for grass 64
15 Main soil groups, thickness of the layers they consist of and the effective root zone for cereals and maize 65
16 Example of a SWACROP input file 67
17 Classification of the ground water table classes 71
18 Overview of soil type, remote sensing relative crop transpiration, SWACROP simulation result, groundwater level and map number for all observation wells on June 20 73
19 Overview of soil type, remote sensing relative crop transpiration, SWACROP simulation result, groundwater level and map number for all observation wells on August 23 74

# PREFACE

By order of the provincial authorities of Drenthe an investigation of the possibilities to apply remote sensing in the construction of a water management strategy was performed in the period 1989-1991. The investigation was carried out by the DLO Winand Staring Centre. From this study (a final report has already been published) it was recommended that it is important to study the possibilities to integrate remote sensing in already existing information structures. In the research presented in this report special attention has been paid to an integrated use of remote sensing and hydrological models.

SUMMARY

For the Province of Drenthe an investigation of the comparability of hydrological modelling and remote sensing on a large scale was performed by the DLO Winand Staring Centre (De Zeeuw, in prep.). For the eastern part of the Province simulations were performed with the model SWACROP. The resulting relative crop transpiration maps were compared to relative crop transpiration images obtained with remote sensing.

The investigation presented in this report consisted of two experiments. The first experiment deals with a detailed comparison of relative crop transpiration values as obtained with remote sensing and according to SWACROP model simulations. In a second study of the possibilities to apply visual interpretation of remote sensing images in hydrological mapping were investigated.

In the growing season of 1989 several remote sensing flights were performed, resulting in a crop type classification map, relative crop transpiration images on June 20 and August 23 and three sets of false colour photographs covering the eastern part of the province (Map numbers 12 Oost and 17 Oost). For June 20 and August 23 maps were composed showing relative crop transpiration values as calculated with the one-dimensional model SWACROP. Simulations were performed for five different agricultural crops: beets, potatoes, maize, cereals and grass. The areal distribution of these crops was derived from a crop type classification map which was derived from the remote sensing data. The one-dimensional model calculations were assigned to soil/hydrological units as derived from existing soil and drainage maps.

Visually both maps corresponded quite well, but the results of a quantitative comparison of the crop transpiration values were disappointing. The input data (drainage class and soil type) used to obtain the areal distribution of the SWACROP simulations appeared to be too schematized. Also crop (either crop type, or crop input parameters in the simulation model) was an important cause of the poor agreement of remote sensing and SWACROP results. A statistical analyses indicated that 79.3% of the differences between the SWACROP and remote sensing results could be explained with the variables "drainage class", "soil type", "crop" and "time", and interactions between these variables. "Drainage class" was indicated as most important followed by "crop", "soil type" and "time" respectively.

With a more detailed input, the SWACROP results were expected to correspond better with the remote sensing values. Therefore in stead of a standard ground water regime (drainage class) measured ground water levels (observation wells IGG-TNO) were used. Additionally on the locations of the observation wells the crop type was checked interpreting the available false colour photographs. For 68 locations simulations were performed.

Investigation of the variation in transpiration values calculated with both methods indicates that SWACROP tends to simulate more extreme relative crop transpiration

values. For the crop maize false colour photographs provide a reliable check of the remote sensing images. Use of these photographs indicated that for maize SWACROP overestimated relative crop transpiration. For the other crop types it was not possible to validate either one of the methods by using false colour photographs. Comparison on individual locations shows that the values calculated with SWACROP and with remote sensing do not correspond very well. The use of more detailed SWACROP input values has not improved the agreement between SWACROP and remote sensing relative crop transpiration values.

The statistical analyses indicated that 48.9 % of the differences between the two methods can be explained with the factors "soil type", "crop", "ground water level" and "time" in order of diminishing importance. Compared to the 79.3 % in the large scale comparison it can be remarked that with the use of improved SWACROP input values a more important part of the differences between both methods have to be subscribed to "noise".
An interaction between soil type and crop seems to exist but the small amount of measurements did not allow stronger statements.

From this experiment could be concluded that studying the individual situation does not answer the question of what causes the deviation between SWACROP and remote sensing satisfactory. It is expected that the differences between the two methods are mainly caused by differences in temporal and spatial scale. Therefore a continuing study should not result in an attempt to optimize the parameters on individual locations. More attention should be paid to the sensitivity of the SWACROP model for small changes in time. Also the variations within soil types should be taken into account, since the soil physical parameters that are linked to the soil type appear to be too standardized. Maybe a stochastic approach of the variation within soil types gives a good start for further research.

In the second experiment visual interpretation of remote sensing images was applied in the validation of the seepage/infiltration map as composed by the Province of Drenthe. The experiment was performed for the northern part of map number 12 Oost. The seepage/infiltration map distinguishes infiltration areas, intermediate areas and seepage areas. The map is based on MODFLOW calculations combined with soil type maps, water table class maps, maps of canals etc. The remote sensing data used in this experiment consisted of false colour photographs and relative crop transpiration images. First a comparison of the relative crop transpiration images and the seepage infiltration map was performed. In seepage areas crops were assumed to show near optimal transpiration whereas in infiltration areas a decreased transpiration was expected. In general patterns of both maps agreeded reasonably well, but there were also areas that did not match the assumptions mentioned above. For two of such areas further research was started. False colour photographs were used to check the relative transpiration images and to obtain information about the spring situation. The MODFLOW input and output information was studied and combined with the other materials used in the composition of the map. Additionally a field survey was carried out. Combination of all the information resulted in a reclassification of the areas and in the decision of the provincial authorities to adapt the existing map using remote sensing images.

From the second experiment it can be concluded that visual interpretation of remote sensing images offers promising opportunities to detect patterns that might not be recognized with more conventional methods. Since there is no linear relationship between crop transpiration and seepage (or infiltration) the use of remote sensing images is restricted to one of indicating remarkable areas. The specific situation of such areas needs to be studied before a reliable decision about classification of such areas can be made.

# 1 INTRODUCTION

Hydrological models for the simulation of transport of soil water or ground water are often applied to evaluate drought damage of agricultural crops. Models have the advantage that evolution in time can be described accurately, but they are limited in that actual field conditions have to be schematized. On the contrary with remote sensing detailed information on regional distribution of crop transpiration can be obtained, but only at acquisition days. Previous research (Thunnissen and Nieuwenhuis, 1989) indicated the meaning of an integrated approach of hydrological modelling and remote sensing for small study areas.

For the Province of Drenthe an investigation of the comparability of hydrological modelling and remote sensing on a larger scale was performed by the DLO Winand Staring Centre (De Zeeuw, in prep.). For the eastern part of the Province simulations were performed with the model SWACROP. The resulting relative crop transpiration maps were compared to relative crop transpiration images obtained with remote sensing. Visually both maps compared quite well, but the results of a quantitative comparison of the crop transpiration values were disappointing. The input data used to obtain the areal distribution of the SWACROP simulations (drainage class and soil type) appeared to be too schematized. Also crop (either crop type, or crop input parameters in the simulation model) was an important cause of the poor correspondence of remote sensing and SWACROP results.

In this study the deviations between the modelling and remote sensing approach have been elaborated. It was decided to use more detailed input data for the SWACROP model. De Zeeuw and Van Middelaar (1991) applied standardized groundwater regimes. In this study measured ground water levels (as far as they were available) were applied. In a second experiment possibilities for visual interpretation of remote sensing images were investigated. A seepage/infiltration map composed with conventional methods has been validated with the available remote sensing images.

In this report some theoretical background about the SWACROP model and the applied remote sensing techniques will be given. Chapter 2 describes the SWACROP model and the input data used in this study. Chapter 3 deals with the applied remote sensing techniques and the available data set. In Chapter 4 attention is paid to the research performed in Drenthe (De Zeeuw, in prep.) and the experiments derived from this investigation. In Chapter 5 the application of visual interpretation of remote sensing images in a hydrological mapping experiment will be discussed. The conclusions derived from the results of the performed experiments will be discussed in Chapter 6.

# 2 SWACROP

Simulations of the evapotranspiration were performed with the model SWACROP (Feddes et al., 1978; Belmans et al., 1983). This model was chosen because it offers good possibilities to work on a detailed scale. Another advantage is the opportunity to link the simulation results to a Geographic Information System (GIS). This is very useful in the comparison between remote sensing and SWACROP results.

SWACROP is a one-dimensional, non-stationary model which simulates soil water content and (evapo)transpiration on a daily basis for the entire growing season. The model uses input data concerning daily periods. As boundary conditions at the soil surface data on rainfall, potential soil evaporation and potential transpiration over 24 h are needed. The soil system is divided into compartments of various thickness. The profile can be split up into layers (containing one or more compartments) with different physical properties (e.g. soil moisture characteristic and hydraulic conductivity). The rooting depth on each day is given as an input, but it may vary in time. At the bottom of system various boundary conditions can be used.

In this chapter the equations applied in the SWACROP model as it was used in this study will be discussed. Additionally a description of the input data used for the simulations is given. Simulations were performed for five different agricultural crops: beets, potatoes, maize, cereals and grass.

## 2.1 Basic flow equation

The basic equation SWACROP uses to describe the flow of water in a heterogeneous soil-root system can be described (Feddes et al., 1978) as:

$$\frac{\partial h}{\partial t} = \frac{1}{C(h)} \frac{\partial}{\partial z} [K(h)(\frac{\partial h}{\partial z} + 1)] - \frac{S(h)}{C(h)} \qquad (1)$$

where h : soil water pressure head (cm);
t : time (d);
C : differential moisture capacity ($d\Theta/dh$) ($cm^{-1}$);
$\Theta$ : volumetric water content;
z : vertical coordinate, with origin at the soil surface, directed positively upwards (cm);
K : hydraulic conductivity ($cm.d^{-1}$);
S : water uptake by plant roots ($d^{-1}$).

## 2.2 Boundary conditions at the top of the system

### 2.2.1 Potential evapotranspiration

Potential evapotranspiration is calculated as:

$$ET^* = f * E_r \tag{2}$$

where $ET^*$ : potential evapotranspiration ($cm.d^{-1}$);
$f$ : crop factor (-);
$E_r$ : reference crop evapotranspiration ($cm.d^{-1}$).

The reference crop evapotranspiration is calculated according to Makkink (1957):

$$E_r = c * \frac{s}{s+\gamma} * \frac{K\downarrow}{\lambda} \tag{3}$$

where $E_r$ : reference crop evapotranspiration ($cm.d^{-1}$);
$c$ : constant (0.65);
$s$ : slope of saturation water vapour pressure at air temperature ($mbar.K^{-1}$);
$\gamma$ : psychrometer constant ($mbar.K^{-1}$);
$K\downarrow$ : global radiation ($W.m^{-2}$)
$\lambda$ : specific latent heat of vaporization ($J.kg^{-1}$).

### 2.2.2 Potential soil evaporation

The SWACROP model offers two methods to calculate the potential soil evaporation: Belmans et al. (1983) and Ritchie and Burnett (Feddes et al., 1978). When the Makkink equation is used to calculate potential evapotranspiration SWACROP uses default Ritchie and Burnett:

$$E^* = 0.00352 * \frac{s}{s+\gamma} * R_n * e^{(-0.39LAI)} \tag{4}$$

where $E^*$ : potential soil evaporation ($cm.d^{-1}$);
LAI : Leaf Area Index ($m^2.m^{-2}$);
$s$ : slope of saturated water vapour temperature and air temperature ($mbar.K^{-1}$);
$\gamma$ : the psychrometer constant ($mbar.K^{-1}$);
$R_n$ : net incoming radiation ($W.m^{-2}$).

The Ritchie and Burnett equation needs a conversion from global radiation to net radiation:

$$R_n = a * K\downarrow - b \qquad (5)$$

where $K\downarrow$ : net radiation ($W.m^{-2}$);
$R_{glob}$ : global radiation ($W.m^{-2}$).

Constants a and b are crop dependent and often not known (except for beets and potatoes). Therefore another method to calculate potential soil evaporation is offered; Belmans equation:

$$E^* = 0.9^{(-0.6LAI)} * ET^* \qquad (6)$$

where $E^*$ : potential soil evaporation ($cm.d^{-1}$);
LAI : Leaf Area Index ($m^2.m^{-2}$);
$ET^*$ : potential evapotranspiration ($cm.d^{-1}$).

For both methods the LAI function of the crop has to be known. But for the crops grass and maize the parameters that describe this function are not accurately known. Thunnissen (1984) related the soil evaporation directly to the open water evaporation and the fraction of soil covered:

$$E^* = (1-S_c) * E_0 \qquad (7)$$

where $S_c$ : fraction of soil covered ($m^2.m^{-2}$);
$E_0$ : open water evaporation according to Penman ($cm.d^{-1}$).

A research group (Feddes, 1987) found an empirical relationship between the Penman open water evaporation and the Makkink reference crop evapotranspiration. The coefficient in this equation varies from 1.17 till 1.31 during the growing season. In this study a constant coefficient of 1.30 has been applied.

$$E_0 = C * E_r \qquad (8)$$

where c: coefficient ($E_r/E_0$).

Combination of equations 7 and 8 results in an equation to calculate potential soil evaporation without knowing the Leaf Area Index function.

$$E^* = (1-S_c) * 1.30 * E_r \quad (9)$$

This linear relationship between soil cover and reference crop evapotranspiration has only been used when the LAI function of the crop was not accurately known (grass and maize). Ritchie and Burnett's equation was used for potatoes and beets. Belmans' method was used for cereals since for this crop the conversion from global to net radiation was not known. Simulation started with the assumption that on the first day of the growing season the unsaturated zone was in equilibrium (elevation head = |pressure head|).

### 2.2.3 Potential crop transpiration

The maximum flux through the canopy can be computed as:

$$T^* = ET^* - E^* \quad (10)$$

where $T^*$ : potential crop transpiration ($cm.d^{-1}$);
$ET^*$ : potential evapotranspiration ($cm.d^{-1}$);
$E^*$ : potential soil evaporation ($cm.d^{-1}$).

This equation is used for potatoes, beets and cereals. Another method has been applied to calculate the potential crop transpiration for maize and grass (Thunnissen, 1984):

$$T^* = S_c * E^*_{100\%} \quad (11)$$

where $S_c$ : fraction of soil covered ($m^2.m^{-2}$);
$E^*_{100\%}$ : potential evapotranspiration at full soil coverage ($cm.d^{-1}$).

Using this equation, the calculation of potential crop transpiration becomes independent of the less accurate calculations of the potential soil evaporation. Furthermore for the crop maize a strong correlation exists between $S_c$ and f.

### 2.2.4 Actual soil evaporation

The actual soil evaporation is calculated according to the method developed by Black et al. (1969). To obtain the actual soil evaporation, the potential soil evaporation is reduced as a function of the number of successive dry days:

$$E_{soil} = \lambda\sqrt{(t+1)} - \lambda\sqrt{t} \quad (12)$$

where $E_{soil}$ : potential soil evaporation ($cm.d^{-1}$);
$\lambda$ : empirical constant (0.35 $cm.d^{-1.5}$);
t : time (d).

SWACROP defines that a dry period ends when the amount of precipitation exceeds 10 mm/d. Thunnissen (1984) adapted this value to 2 mm/d. This value is used for the crops grass and maize.

### 2.2.5 Actual crop transpiration

The actual crop transpiration depends on rooting depth and the capacity of the root system to extract water. Calculations are based on the Sink term (Feddes et al., 1978). The Sink term describes the extraction of water by the root system for each soil compartment.

$$S(h) = \alpha(h) * S_{max} \qquad (13)$$

where S(h) : actual volume of water taken up by roots per unit volume of soil per unit time ($d^{-1}$);
$\alpha(h)$ : prescribed function of soil water pressure head (-);
$S_{max}$ : maximum possible volume of water taken up by roots per unit volume of soil per unit time ($d^{-1}$).

Figure 1 shows the general shape of $\alpha$. Root water uptake is zero above $h_1$ and below $h_4$ (wilting point), maximal between $h_2$ and $h_3$ with a linear relationship assumed from $h_1$ and $h_2$ and from $h_3$ and $h_4$.

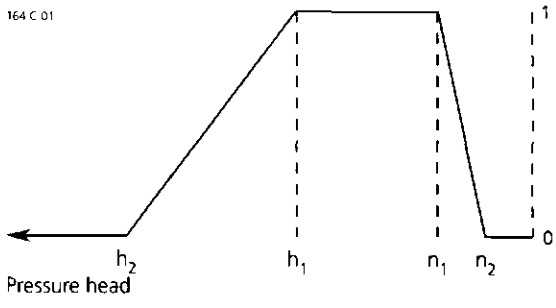


***Fig. 1 General shape of the dimensionless Sink term variable $\alpha$, as a function of the soil water pressure head, h (Belmans et al., 1983)***

The definition of $\alpha(h)$ is different for each crop and will be described in par. 2.4.4. The maximum possible root extraction rate can be described as:

$$S_{max} = \frac{T^*}{|z_r|} \qquad (14)$$

where $T^*$ : potential transpiration rate ($cm.d^{-1}$);
$z_r$ : bottom of the (effective) root zone (cm).

The actual crop transpiration is calculated as:

$$T_{act} = \sum S(h) \qquad (15)$$

where $T_{act}$ : actual crop transpiration ($cm.d^{-1}$).

2.2.6 Relative crop transpiration

Relative crop transpiration is not a direct SWACROP output value. It is calculated as:

$$E_{rel} = \frac{T_{act}}{T^*} \qquad (16)$$

where $E_{rel}$ : relative crop transpiration;
$T^*$ : potential transpiration rate ($cm.d^{-1}$);
$T_{act}$ : actual crop transpiration ($cm.d^{-1}$).

2.3 Boundary conditions at the bottom of the system

At the bottom of the soil system SWACROP offers various possibilities of boundary conditions. In this study a measured ground water level is used. This means that the system is partly saturated. SWACROP calculates the flux between saturated and unsaturated zone.

2.4 Input data

This paragraph contains an overview of the data used for the SWACROP simulations. An important part of the parameters has been calibrated during the Remote Sensing Project Drenthe. The growing season that has been simulated in this study covers a period between 1 march until 1 october 1989 (Julian day numbers 60 until 273). For

each crop the simulation starts on the day of sowing and ends on the day of harvesting.

### 2.4.1 Meteorological data

Evapotranspiration calculations according to Makkink need 24-hour data on average temperature (°C), global radiation ($W.m^{-2}$), and relative humidity. These data were obtained from the KNMI (Royal Dutch Meteorological Institute). Precipitation data (24 h) were obtained from a local meteorological station. To find the most appropriate meteorological station for the precipitation data a network of "Thiessen polygons" was set up. For map number 12 Oost precipitation data of the meteorological station Gieterveen and for map number 17 Oost precipitation data from meteorological station Zweeloo were used. The remaining meteorological data (temperature, relative humidity and global radiation) were obtained from the major station Eelde.

### 2.4.2 Ground water levels

Location of the observation wells and the measured ground water levels were obtained from IGG-TNO and the Province of Drenthe. Data were available on a monthly or two-weekly basis (around the $14^{th}$ and $28^{th}$ of each month).

### 2.4.3 Soil and hydrology

For each location the soil type has been derived from a generalized soil map. This soil map was developed for modelling purposes in the "Tussen-10-plan" (Bannink and Stoffelsen, 1984). The soil types distinguished on regular soil maps of the Province of Drenthe were generalized to 22 main groups. Annex 1 shows the generalized soil map for the map numbers 12 Oost and 17 Oost. A global description of the main groups is given in Annex 2. Each main group is a composition of several layers. Every layer has its own soil hydraulic properties (e.g. soil-moisture characteristic and hydraulic conductivity). In total 24 different layers are distinguished. Annex 3 contains for each crop a table with the main soil groups and the thickness of the layers of these groups they consist of.

### 2.4.4 Crop

*Growing season*
Simulations were performed for five different agricultural crops: potatoes, beets, grass, maize and cereals. The days of sowing and harvesting of these crops are presented in Table 1. These data are obtained from the experimental farm "De Kooienburg". De

Kooienburg is situated on a loamy soil and therefore sensitive to water excess in spring. This has been taken into account at the interpretation of these data. For each crop simulation starts at the day of sowing and ends on the harvesting day. For grass the "growing season" was set on the period between Julian day number 60 until 273.

*Table 1 Simulated crops with their sowing and harvesting days (Julian day numbers, 1989)*

| Crop | Sowing | Harvest |
|---|---|---|
| **Potatoes** | **91** | **253** |
| **Maize** | **124** | **274** |
| **Beets** | **91** | **278** |
| **Cereals** | **91** | **222** |
| **Grass** | **-** | **-** |

*Leaf Area Index*

The Leaf Area Index (LAI) is related to the fraction of soil covered ($S_c$ in %):

$$LAI = a * S_c + b * S_c^2 + c * S_c^3 \qquad (17)$$

The factors a, b and c are different for each crop. The values for the crops as used in this study are given in Table 2 (Wesseling, 1991).

*Table 2 Values for the crop dependent constants a, b, and c used in the Leaf Area Index function*

| Crop | a | b | c |
|---|---|---|---|
| **Potatoes** | **2.5000** | **1.6000** | **0.9000** |
| **Maize** | **0.0280** | **2.9100** | **0.9570** |
| **Beets** | **4.6785** | **-18.0386** | **19.2525** |
| **Cereals** | **0.0593** | **- 0.4512** | **5.8143** |
| **Grass** | **6.3877** | **-17.7030** | **16.0697** |

*Fraction of soil covered*

The percentage of soil covered by potatoes was profoundly studied by Van der Schans et al. (1984). Figure 2 shows a standard curve as developed for potatoes for agri-industrial production. Additionally an experimental curve (Van der Schans et al., 1984), and a curve that was used in the simulations (De Zeeuw, 1991) is presented in this figure. The fraction of soil covered for grass was presumed to be 100% over the complete simulation period. The assumed soil coverage curves for beets, maize and cereals are shown in Figure 3 (Wesseling, 1991).

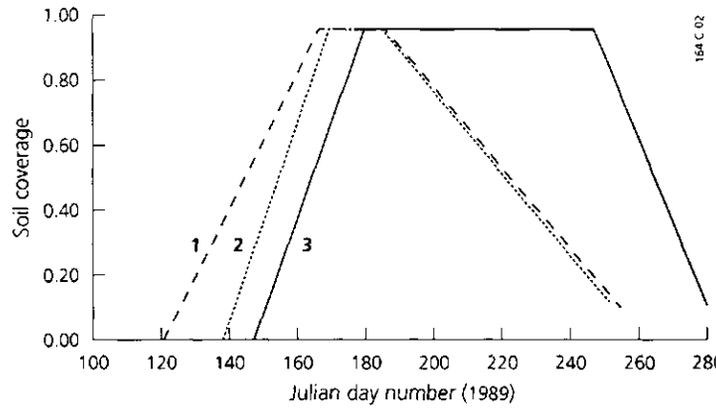


1. Simulated soil coverage
2. Measured soil coverage
3. Soil coverage for Drenthe

***Fig. 2 Fraction of soil covered for a standard growing season for potatoes***

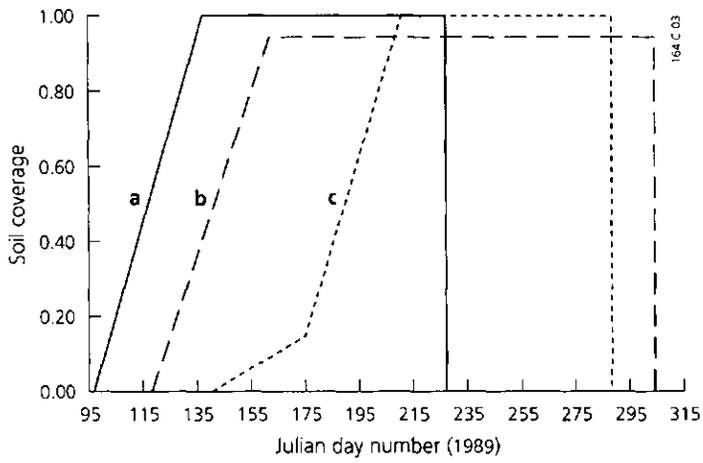


a. Soil coverage for cereals
b. Soil coverage for beets
c. Soil coverage for maize

***Fig. 3 Fraction of soil covered for a standard growing season for cereals, beets and maize***

*Crop factor*

The crop factors used in the Makkink evapotranspiration calculations are presented in Table 3 (Feddes, 1987).

*Table 3 The crop factors per decade and the corresponding input days*

| Month | April | | | May | | | June | | | July | | | August | | | September | | |
|---|---|---|---|---|---|---|---|---|---|---|---|---|---|---|---|---|---|---|
| Decade | I | II | III | I | II | III | I | II | III | I | II | III | I | II | III | I | II | III |
| JDN | 91 | 100 | 110 | 121 | 131 | 141 | 152 | 162 | 172 | 182 | 192 | 202 | 213 | 223 | 233 | 244 | 254 | 264 |
| Potatoes | - | - | - | - | 0.7 | 0.9 | 1.0 | 1.2 | 1.2 | 1.2 | 1.1 | 1.1 | 1.1 | 1.1 | 1.1 | 0.7 | - | - |
| Maize | - | - | - | 0.5 | 0.7 | 0.8 | 0.9 | 1.0 | 1.2 | 1.3 | 1.3 | 1.2 | 1.2 | 1.2 | 1.2 | 1.2 | 1.2 | 1.2 |
| Beets | - | - | - | 0.5 | 0.5 | 0.5 | 0.8 | 1.0 | 1.0 | 1.2 | 1.1 | 1.1 | 1.1 | 1.2 | 1.2 | 1.2 | 1.1 | 1.1 |
| Cereals | 0.7 | 0.8 | 0.9 | 1.0 | 1.0 | 1.0 | 1.0 | 1.2 | 1.2 | 1.0 | 0.9 | 0.8 | 0.6 | - | - | - | - | - |
| Grass | 1.0 | 1.0 | 1.0 | 1.0 | 1.0 | 1.0 | 1.0 | 1.0 | 1.0 | 1.0 | 1.0 | 1.0 | 1.0 | 1.0 | 0.9 | 0.9 | 0.9 | 1.1 |

*Rooting depth and root growth*

Since water extraction is related to the plant root system it is of great importance that the root system is correctly described. SWACROP uses two factors in this description; maximum rooting depth and growth rate of the roots. Both factors depend on soil type and ground water level. Roots from potatoes for instance have only small capacity to penetrate into the soil. Once a more dense layer is reached, root growth (vertically) stops. Therefore the effective root zone is often set at 25 cm while it can reach 90 cm in more favourable situations. Annex 3 gives the depth of the effective root zone of all simulated crops for each soil type (main group). Table 4 shows the growth rate of the roots as used for the simulated crops.

*Table 4 Growth rate of the rooting system during the growing season and the maximum rooting depth for potatoes, maize, beets, cereals and grass*

| Crop | Root growth ($cm.d^{-1}$) | Max. rooting depth (cm) |
|---|---|---|
| Potatoes | 1,25 | 20-50 |
| Maize | 1 | 20-75 |
| Beets | 1,25 | 20-50 |
| Cereals | 1 | 20-75 |
| Grass | constant | 15-30 |

*Water uptake by the root system*

Water uptake by the root system can be described with the "Sink term" (Feddes et al., 1978). Figure 4 shows the reduction factor $\alpha$ for different potential transpiration rates. In Table 5 the pressure heads used to describe the reduction factor $\alpha$ are shown.

*Table 5 Pressure heads (cm) that describe the reduction factor α for potatoes, maize, beets, cereals and grass*

| Crop | h1 | h21 | h3h | h31 | h4 |
|---|---|---|---|---|---|
| **Potatoes** | **-10** | **-25** | **-320** | **-600** | **-16 000** |
| **Maize** | **-15** | **-30** | **-325** | **-600** | **- 8 000** |
| **Beets** | **-10** | **-25** | **-320** | **-320** | **-16 000** |
| **Cereals** | **0** | **- 1** | **-500** | **-900** | **-16 000** |
| **Grass** | **-10** | **-25** | **-200** | **-800** | **- 8 000** |

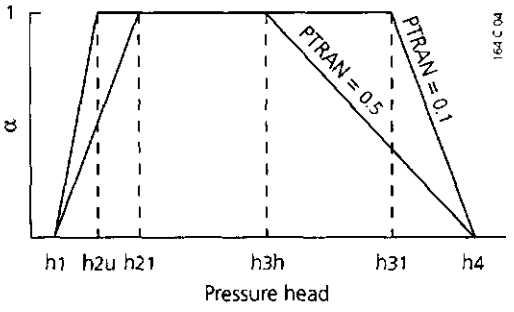


*Fig. 4 Shape of the reduction factor α in the Sink term as a function of pressure head h (Feddes et al., 1978)*

*Interception function*
The interception function describes that part of the precipitation that actually reaches the soil surface. In this study the standard formula SWACROP offers was used:

If precipitation > 0.2 cm.d$^{-1}$:

$$INTCEP = S_c * 0.19 \quad (18)$$

If precipitation < 0.2 cm.d$^{-1}$:

$$INTCEP = S_c * P^{(0.516 - 0.1787 * (P - 0.0593))} \quad (19)$$

where INTCEP: calculated interception (cm.d$^{-1}$);
$S_c$ : fraction of soil covered (-);
P : precipitation (cm.d$^{-1}$).

2.4.5 Additional input data

The residual input parameters, needed for the simulation process are described in this paragraph. Annex 4 shows an example of an input file as used in this study. The

Makkink formula is used to calculate evapotranspiration. Boundary condition at the soil surface is a measured ground water level. The soil system is divided into several horizons with different soil hydrological properties, and in 40 compartments with variable thickness (20 * 5 cm, 10 * 10 cm and 10 * 20 cm). Figure 5 shows a scheme of the soil system and the calculated fluxes as applied in this study.

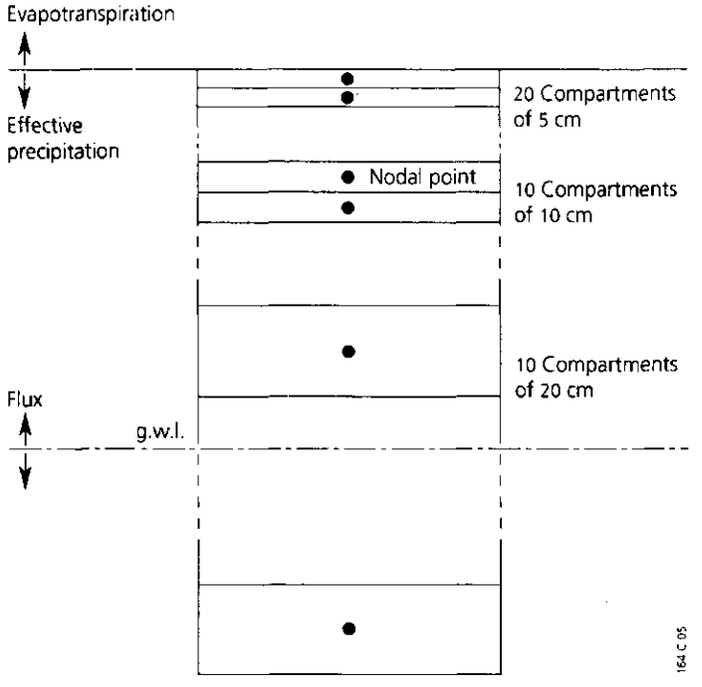


***Fig 5 Scheme of the soil system and the calculated fluxes***

# 3 REMOTE SENSING

## 3.1 Data

In the framework of the Remote Sensing Project Drenthe a very extensive set of data was collected. In the growing season of 1989 three remote sensing flights were performed. On June 20 and August 23 digital reflectance and thermal infrared images were obtained with a Deadalus scanner simultaneously with false colour photographs. On April 2 only false colour images were made. Additionally an image of the French SPOT satellite, May 22, was used. Ground truth data were collected on all flight days. On April 2 (colour) pictures were taken to detect water excess and drought stress patterns in the top soil. On June 20, a crop type inventarisation was made. Furthermore reference crop temperature was measured. The same data were collected on August 23. The August ground truth data were used to calibrate the crop type classification and the evapotranspiration mapping. Table 6 shows the data used in this study and their applications.

*Table 6 Data and applications in the Remote Sensing Project Drenthe*

| Date (1989) | RS techniques | Application |
|---|---|---|
| April 2 | False colour photographs | Water excess in spring |
| May 22 | SPOT MSS[1] | Land use classification |
| June 20 | Deadalus MSS, IRLS[2] | Land use classification and |
| | False Colour photographs | evapotranspiration mapping |
| August 23 | Deadalus MSS, IRLS | Land use classification and |
| | False Colour photographs | evapotranspiration mapping |

[1] Multi Spectral Scanning
[2] Infra Red Line Scanning

## 3.2 False colour photographs

Colour infrared film is manufactured to record green, red and the photographic portion (0.7-0.9 μm) of the near infrared scene energy in its three emulsion layers. This results in a false colour film in which blue images result from object reflecting primarily green energy, green images result from objects reflecting primarily red energy and red images result from objects reflecting primarily in the near infrared portion of the spectrum. (Lillesand and Kiefer, 1987). For example vegetation reflects infrared energy much more than green energy and it generally appears in various tones of red on false colour film.

In this study the available set of false colour photographs (April, June and August) was used to check the automatic crop type classification at the location of the observation wells. Table 7 gives an overview of the condition of the crops at the

flight dates. Using this scheme in combination with the typical red colour of the different crops gives a reliable verification of the crop type classification.

*Table 7 Condition of different crops on the flight days*

| Crop | April 2 | June 20 | August 23 |
|---|---|---|---|
| Grass | Vegetation | Vegetation | Vegetation |
| Cereals (summer) | Bare soil | Vegetation | Bare soil |
| Cereals (winter) | Vegetation | Vegetation | Bare soil |
| Potatoes | Bare soil | Vegetation | Vegetation/bare soil |
| Beets | Bare soil | Vegetation | Vegetation |
| Maize | Bare soil | Bare soil | Vegetation |
| Peas | Bare soil | Vegetation | Vegetation |
| Forest | Vegetation | Vegetation | Vegetation |

Another application of the false colour photographs is based on the difference in reflection of a healthy vegetation and a stressed vegetation. Healthy vegetation shows a much deeper red colour than stressed vegetation. This offers good possibilities to detect drought stress patterns.

## 3.3 Airborne Multispectral Scanning (MSS) and Infrared Line Scanning (IRLS)

The multi-spectral images of the Province of Drenthe were made with a Deadalus scanner. This electro-optical system registers electromagnetic radiation in the range of 0.3-14 μm in 12 bands. Table 8 contains an overview of the scanner data, the spectral bands that were used, and the ground resolutions.

*Table 8 Available scanner data, the spectral bands and the ground resolution*

| Scanner type | Band (μm) | Ground resolution |
|---|---|---|
| Deadalus, MSS | 5 0.55- 0.60 | 10 * 10 m[1] |
| | 7 0.65- 0.69 | |
| | 9 0.80- 0.89 | |
| Deadalus, IRLS | 12 8.50-13.50 | 10 * 10 m[1] |
| SPOT, MSS | 1 0.50- 0.59 | 20 * 20 m |
| | 2 0.62- 0.68 | |
| | 3 0.79- 0.89 | |

[1] The spatial resolution of the image was 12.5 * 12.5 m,
[2] After resampling 10 * 10 m

A rotating mirror moves the field of view of the scanner along a scan line perpendicular to the flight direction. The forward motion of the aircraft advances the viewed strip between scans, causing a two dimensional image data set to be recorded (Lillesand and Kiefer, 1987). In Figure 6 a schematic illustration of a multi spectral scanner system operation is given.

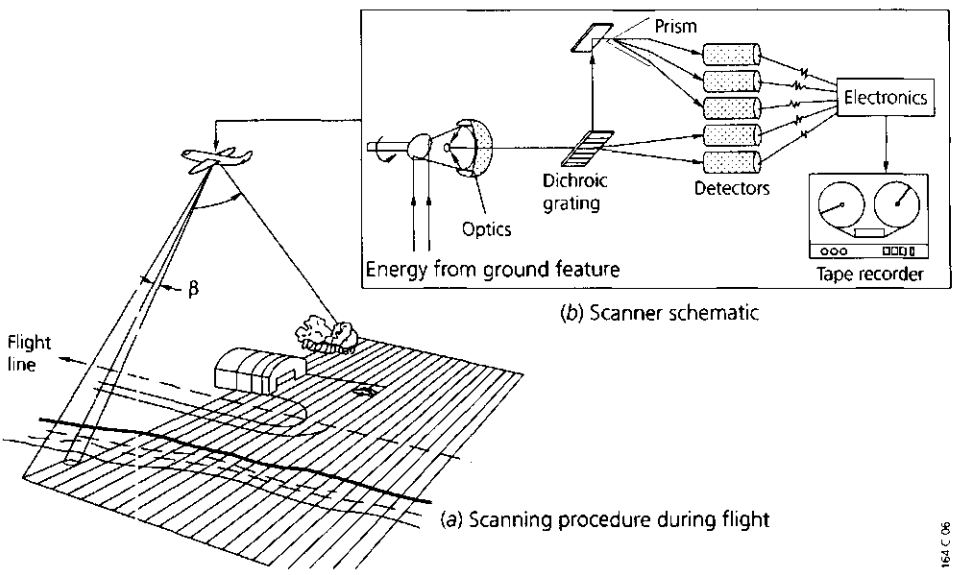


*Fig. 6 Multispectral scanner system operation (Lillesand and Kiefer, 1987)*

## 3.4 Crop type classification

A multi-temporal crop type classification was performed for the eastern part of the province (map numbers 12 Oost and 17 Oost). This classification was based on the Maximum Likelihood (MLHD) criterion. The final crop type classification was a result of several partial classifications:

1 The SPOT-May image was used to make a distinction between early crops (grass and cereals) and (still) bare soil, based on a respectively high and low Vegetation Index. A relatively low vegetation index belongs to the land use classes potatoes, beets, peas, and bare soil (including open water and built up area). The Vegetation Index can be described as:

$$VI = (IR - R) / (IR - R) \qquad (20)$$

where IR : Reflectance in the infrared part of the spectrum
R : Reflectance in the red part of the spectrum

2 For the area with a low vegetation index in May a classification was performed using the Deadalus June images. Combination of SPOT-May (bands 1, 2 and 3) and the Deadalus-June (bands 5, 7 and 9) data resulted in the distinction of 5 classes: Grass/cereals, deciduous forest, coniferous forest, peas, and bare soil (open water and build up area included).

3 This last classification was performed to verify former classifications. Deadalus data (band 5, 7 and 9) of August 23 were used. A distinction was made between vegetation, bare soil (again including open water and built up area) and clouds.

The crop maize caused a lot of problems in the automatic classification because its spectral signature was similar to that of other crops on the measurement dates. Therefore with the use of false colour photographs of June and August maize fields were detected interactively. The fields were digitized and combined with the classification results.

The final crop type classification result was combined with geographical information on built up area, infrastructure and open water. This information was obtained from (digital) topographic maps (1 : 50,000). In Annex 1, Figure 15 the final crop type classification is presented.

## 3.5 Evapotranspiration mapping

By combining the surface energy balance equation with the vertical transport equation for sensible heat a relationship between latent heat flux LE and crop temperature can be derived (Soer, 1980).

$$LE = \rho c_p \frac{(T_a - T_c)}{r_{ah}} + (1 - \alpha)R_s + \varepsilon(R_l - \sigma T_c^4) - G \qquad (21)$$

where LE : latent heat flux ($W.m^{-2}$);
$\rho$ : density of moist air ($kg.m^{-2}$);
$c_p$ : specific heat of moist air ($J\ kg^{-1}.K^{-1}$);
$T_a$ : air temperature at a reference height above the crop (K);
$T_c$ : crop temperature (K);
$r_{ah}$ : turbulent diffusion resistance for heat transport ($s.m^{-1}$);
$R_s$ : incoming short wave radiation flux ($W.m^{-2}$);
$\alpha$ : reflection coefficient of the crop (-);
$\varepsilon$ : emission coefficient of the crop (-);
$R_l$ : long wave sky radiation flux ($W.m^{-2}$);
$\sigma$ : The Boltzmann constant ($W.m^{-2}.K^{-4}$);
G : heat flux into the soil ($W.m^{-2}$).

With the use of this equation the instantaneous evapotranspiration flux of a crop can be calculated from the temperature of the crop. To convert instantaneous crop temperatures into 24 hour estimates of evapotranspiration $LE^{24}$ Soer (1980) developed the TERGRA model (Soer, 1977). Computation of evapotranspiration rates from thermal images with the aid of the TERGRA model is rather complicated because of the large number of input parameters that is required.

Therefore Nieuwenhuis et al. (1985) used the method of Jackson et al. (1977) to develop a simplified method to relate actual 24 hour evapotranspiration and the midday temperature difference between a crop that is transpiring under restricted soil water conditions ($T_c$) and one that is transpiring under optimal soil water conditions ($T_c^*$) according to:

$$LE^{24} = LE_p^{24} - B'(T_c - T_c^*) \qquad (22)$$

where $LE^{24}$ : actual 24 hour transpiration ($W.m^{-2}$);
$LE_p^{24}$ : potential 24 hour transpiration ($W.m^{-2}$);
$B'$ : calibration constant ($W.m^{-2}.K^{-1}$);
$T_c$ : temperature of a crop transpiring under restricted soil water conditions (K);
$T_c^*$ : temperature of a crop transpiring under optimal conditions (K).

The factor B' is a calibration constant. Results with the TERGRA model show that constant B' becomes less dependent on meteorological conditions when evapotranspiration differences in equation (22) are replaced by relative evapotranspiration values (Thunnissen and Nieuwenhuis, 1989):

$$\frac{LE^{24}}{LE_p^{24}} = 1 - B^r(T_c - T_c^*) \qquad (23)$$

where $B^r$: calibration constant ($K^{-1}$).

Calibration constant $B^r$ equals $B'/LE_p^{24}$. By means of equation (23) differences in radiation temperature of a crop derived from thermal images can be directly transformed into reductions in 24 hour evapotranspiration. From TERGRA calculations it was found that $B^r$ was linearly related to the wind velocity at a height of 2 m above a flat and open area according to :

$$B^r = a + b * u(2) \qquad (24)$$

where u(2) : wind velocity at a height of 2 m ($m.s^{-1}$);
a : regression coefficient ($K^{-1}$);
b : regression coefficient ($K^{-1}.m.s^{-1}$).

Factors a and b depend on crop type and crop height. The values for a and b used in this study are given in Table 9.

*Table 9 Values of regression coefficients and for different crops at standard heights*

| Crop | Height (cm) | a ($K^{-1}$) | b ($K^{-1}.m.s^{-1}$) |
|---|---|---|---|
| Grass | 10 | 0.050 | 0.068 |
| Grass | 20 | 0.050 | 0.081 |
| Potatoes | 60 | 0.050 | 0.092 |
| Beets | 60 | 0.050 | 0.092 |
| Cereals | 100 | 0.090 | 0.144 |
| Maize | 200 | 0.100 | 0.185 |

By combination of the crop type map and the thermal image, using the equations discussed before, the thermal image was automatically converted into a relative crop transpiration map. For short grass no evapotranspiration values were computed. Because short, recently mowed grass has an incomplete soil cover, the observed thermal radiation temperature was to a large extent determined by the relative high radiation temperature of the bare parts of the soil. Due to the height and roughness of trees heat is easily exchanged with the atmosphere, so that reduction in evapotranspiration of trees cannot reliably be derived from thermal infrared images. Therefore evapotranspiration of forests was not calculated either. In the Figure 7 the relative crop transpiration maps for June 20 and August 23 respectively are presented.

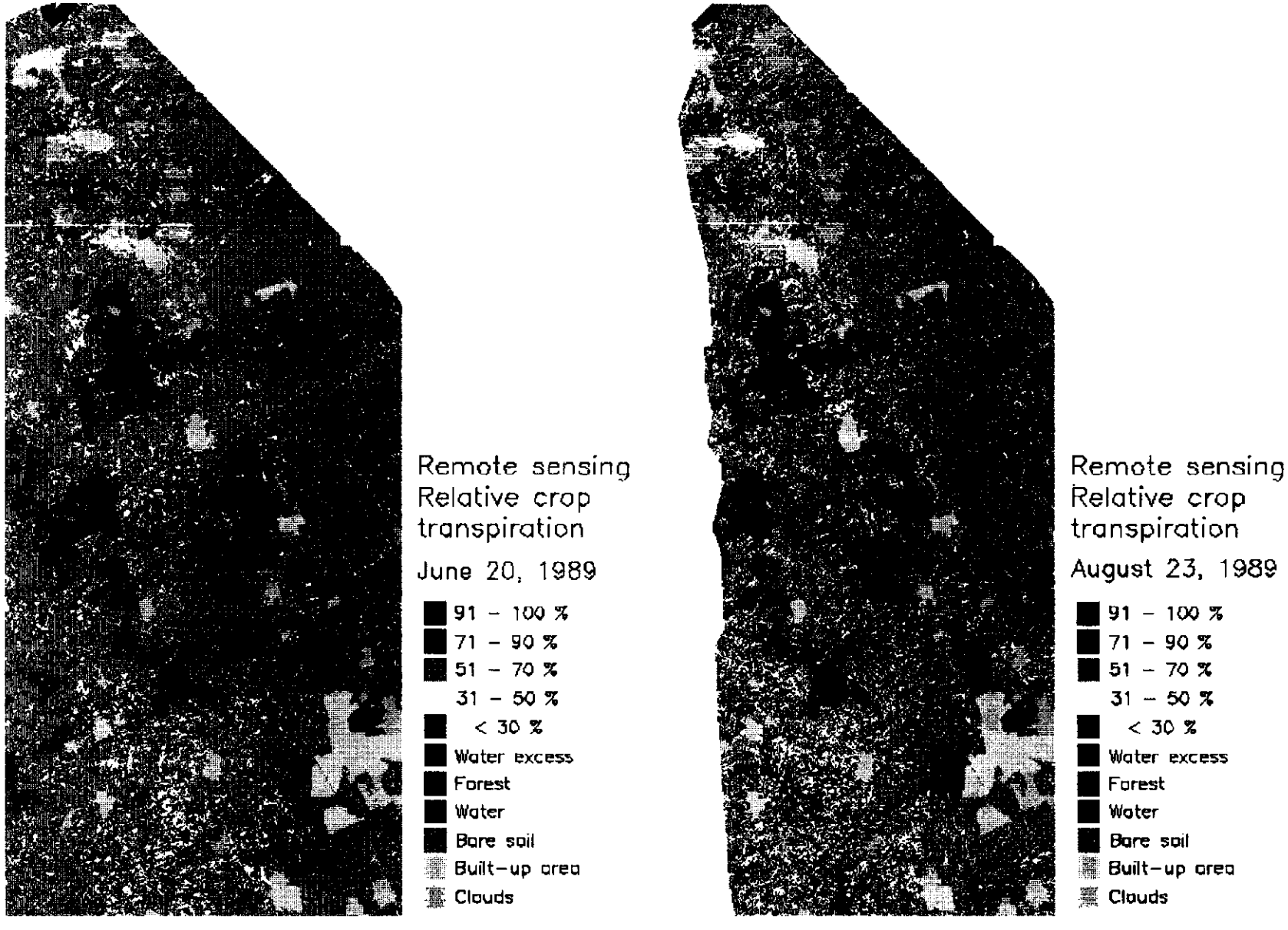


*Fig. 7 Relative crop transpiration map for map numbers 12 Oost and 17 Oost on June 20 and August 23, 1989 (De Zeeuw, 1991)*

# 4 COMPARISON OF REMOTE SENSING AND SWACROP RELATIVE CROP TRANSPIRATION VALUES

This experiment was a continuation of the large scale comparison of both remote sensing and SWACROP relative crop transpiration values for the Province of Drenthe. Before describing the experiment performed in this study a short description of the study area and a summary of the preceding investigation will be given.

## 4.1 Description of the study area

The study area is situated in the eastern part of the Province of Drenthe (map numbers 12 Oost and 17 Oost), The Netherlands. In the study area several different soil-hydrological units and landscape types occur. Figure 8 shows the two map numbers and their landscape types. The Drenths plateau consists of reclaimed land, essen (human effected sandy soils) and brook valleys. The Hondsrug, east of the Drenths plateau is a relatively high area (up to 20 m above sea level) with mainly sandy (human effected) and reclaimed soils. Here ground water levels are somewhat deeper below the soil surface, except for the brook valleys that cross the Hondsrug. On its east side the Hondsrug changes quite abruptly into the Hunze valley. The Hunze valley is a brook valley with mainly histic and peaty soils with shallow groundwater levels. An important part of this area is drained by the river Hunze. At the eastern parts of the maps the landscape changes into the "Veenkoloniën". The Veenkoloniën consists of peaty and histic soils and concerns reclaimed land.

## 4.2 Large scale comparison of remote sensing and SWACROP relative crop transpiration values

The investigation dealing with the comparability of remote sensing and SWACROP relative crop transpiration values was performed as a part of the Remote Sensing Project Drenthe. In this project the possibilities for remote sensing to support in the water management policy of the Province of Drenthe were studied.
In the growing season of 1989 several remote sensing flights were performed, resulting in a crop type classification map, relative crop transpiration images for June 20 and August 23 and a set of false colour photographs covering the eastern part of the province (Map numbers 12 oost and 17 oost). For the same dates images were created from the relative crop transpiration values simulated with the one-dimensional model SWACROP. Simulations were performed for five different agricultural crops: beets, potatoes, maize, cereals and grass. The areal distribution

of these crops was derived from a crop type classification map. This map was derived from the remote sensing data. To extrapolate the calculated values a combination of a soil map and a drainage class map was used

For modelling purposes the soil map used in this study has been generalised to 22 main groups (according to Bannink and Stoffelsen, 1984). The drainage class map was derived from a water table class map by joining resembling water table classes to four drainage classes. Water table classes are based on the mean highest and mean lowest groundwater table, representing the average winter and summer water table in a year with an average precipitation and evaporation. In Annex 5 an overview is given of the existing groundwater table classes.

Visual comparison of the remote sensing and SWACROP relative crop transpiration maps showed that striking patterns like drought stress patterns were clearly visible on both maps. Also general landscape patterns e.g. brook valleys, the Veenkoloniën and the Hondsrug could be recognized easily. A more quantitative comparison displayed a lot of deviations between the relative crop transpiration values calculated with both methods. In general SWACROP simulated more extreme values (either near optimal transpiration or severe drought stress) than remote sensing did. For sandy soil types SWACROP often simulated strongly reduced transpiration, whereas on peaty soils optimal transpiration rates dominated. A statistical analyses based on simultaneous regression techniques indicated that 79.3% of the deviations between SWACROP and remote sensing results could be explained through the factors "drainage class", "crop", "soil type" and "time" and the interactions between those factors. "Drainage class" and "crop" respectively, were the most important factors in the explanation of the differences between remote sensing and SWACROP results (De Zeeuw, 1991).

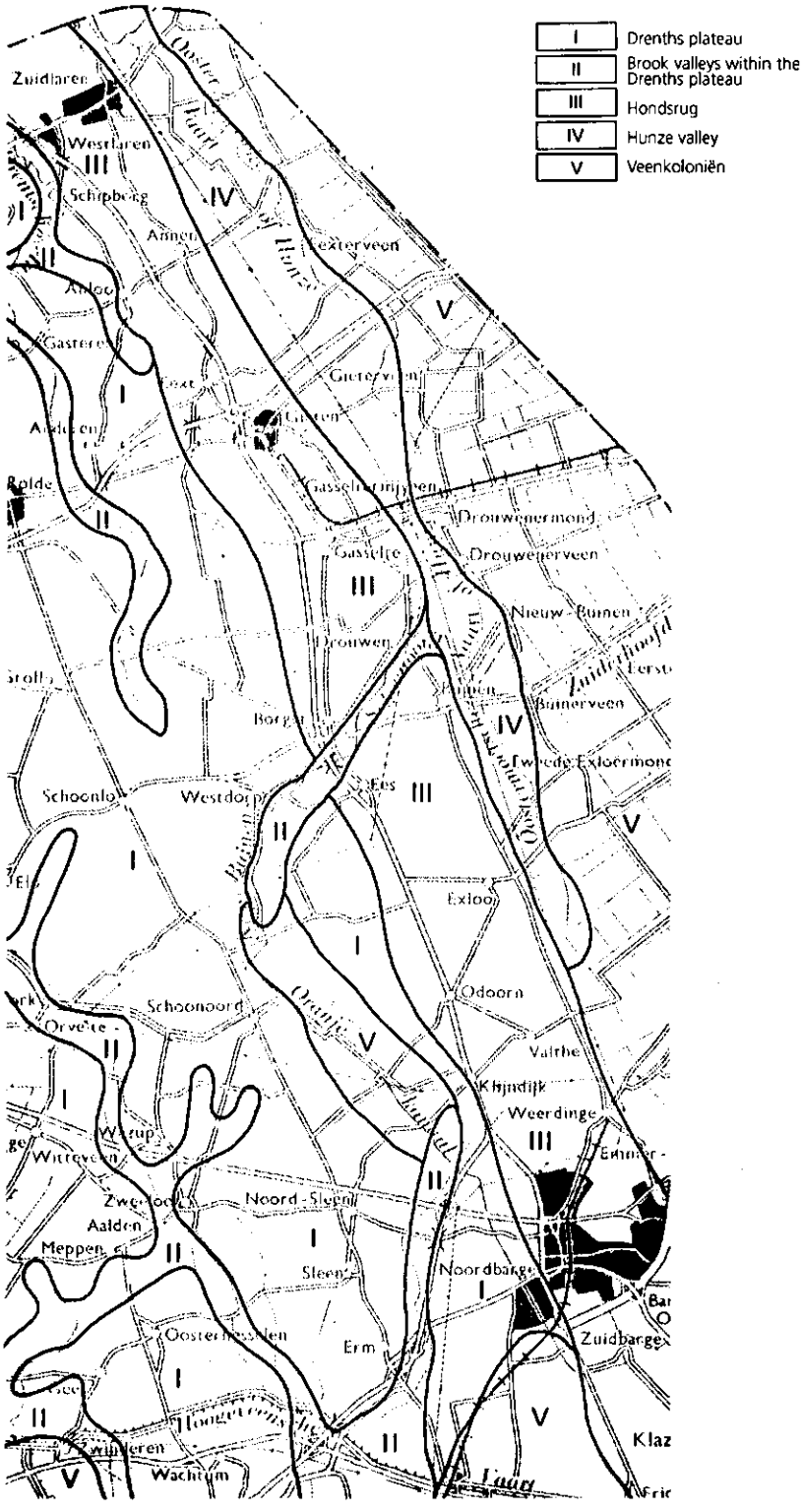


*Fig. 8 Situation of map numbers 12 Oost and 17 Oost in the Province of Drenthe*

## 4.3 Detailed comparison of SWACROP and remote sensing relative crop transpiration values

As a continuation of the large scale comparison another approach was chosen. With a more detailed input, the SWACROP results were expected to compare better with the remote sensing values. The use of more precise SWACROP input corresponds with the results obtained in the Oost Gelderland Project (Thunnissen, 1984). In this project a comparison was made between SWATRE (a previous release of SWACROP; Belmans e.a., 1983) and remote sensing crop transpiration values. The SWATRE input consisted mainly of measured values (groundwater level, soil hydraulic properties, crop type) and the simulation results compared satisfactory with the remote sensing crop transpiration values.

This more detailed approach signified the use of a more precise lower boundary condition and a correct crop type input. In stead of a standardized groundwater regime (drainage class) measured groundwater levels were used as lower boundary condition. Groundwater levels were obtained from monthly or two-weekly measurements in observation wells (IGG-TNO). The locations of these observation wells were selected with topographic maps and false colour photographs. The use of measured groundwater levels as input data implemented that the comparison between SWACROP and remote sensing values was restricted to the location of the observation well. At the location of the observation wells the crop type classification map was checked with false colour photographs. Since no measured values of soil physical properties were available for the study area, standard values as described by Bannink and Stoffelsen (1984) were used. After the selections 68 locations remained. For these locations simulations were performed. A comparison was made between the simulated relative crop transpiration values and the values obtained with remote sensing.

## 4.4 Results and discussion

### 4.4.1 Variation in crop transpiration values

The relative crop transpiration results of both methods were divided in five transpiration classes: 0-30%, 31-50%, 51-70%, 71-90% and 91-100%. In Figure 9 the appearance in the different transpiration classes for both methods is given.

The distribution over the different transpiration classes is more equal for remote sensing than for SWACROP results. The SWACROP values are concentrated in the two most extreme classes (0-30% and 91-100%). In June the SWACROP values are concentrated in the 90-100% transpiration class. In august also part of the SWACROP values vary from 0 to 30%. (De Zeeuw, 1991). For the different crops a similar comparison was made, shown in figure 10.

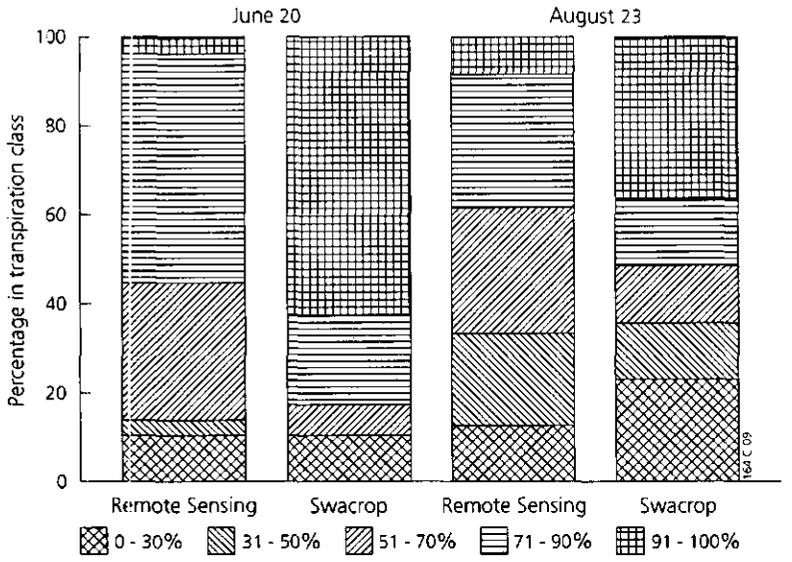


*Fig. 9 Relative crop transpiration distribution according to remote sensing and SWACROP simulation results on June 20 and August 23 for map numbers 12 Oost and 17 Oost*

For beets the distribution over the different transpiration classes shows that SWACROP simulates more reduced transpiration values than remote sensing does. For grass over 40% of the SWACROP values are situated in the 91-100% transpiration class, whereas this class does not even exist for the remote sensing results. The same situation occurs for maize where the difference between SWACROP and remote sensing is even more extreme.

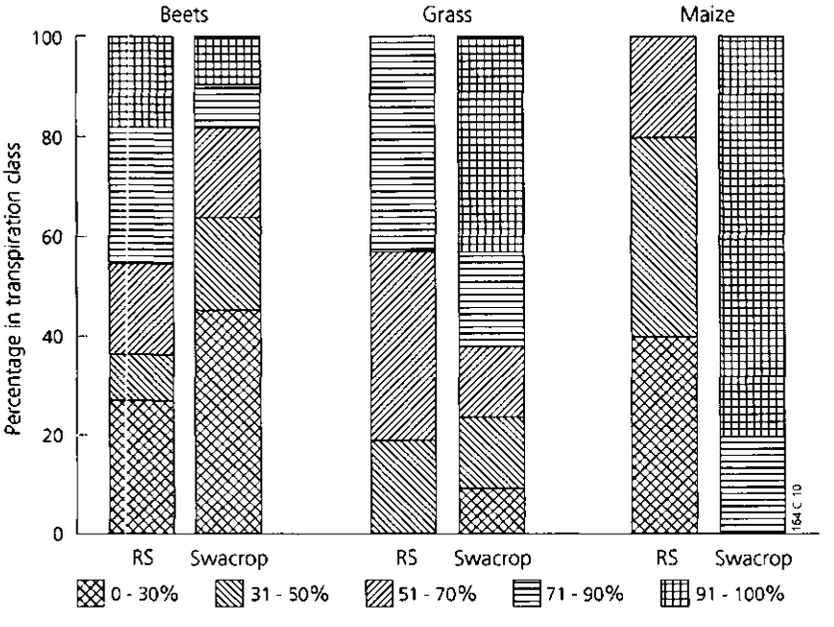


*Fig. 10 Relative crop transpiration distribution according to remote sensing and SWACROP simulation results for beets, grass and maize on August 23 (map numbers 12 Oost and 17 Oost)*

A possible explanation for the fact that SWACROP often simulates rather extreme transpiration values was found by Thunnissen (1984). In certain circumstances the SWATRE model is very sensitive to small changes in input data. (e.g. small changes in groundwater level). In a period of three days calculated crop transpiration values can diminish to one third of the original value (Thunnissen, 1984). Remote sensing is based on measurements of only one moment. Comparison of remote sensing and SWACROP on that specific moment might imply that this small changing period is missed.

### 4.4.2 Comparison on individual locations

As it is indicated in par. 4.4.1 remote sensing transpiration values deviate from the SWACROP transpiration values. The scatter in Figure 11 shows the deviations between both methods. Compared to the results obtained by De Zeeuw (1991) there is no real improvement in the correspondence of the relative crop transpiration values calculated with both methods. This is in contradiction with the expectation that a more precise SWACROP input results in a better agreement between the results of the SWACROP and the remote sensing approach. To explain the deviations between the SWACROP and remote sensing results, the relative crop transpiration values on the individual locations were studied more precisely. In Annex 6 the simulation results as well as the remote sensing values are given for each observation well. Before investigating what might cause the deviations between remote sensing and SWACROP values a few remarks should be made.

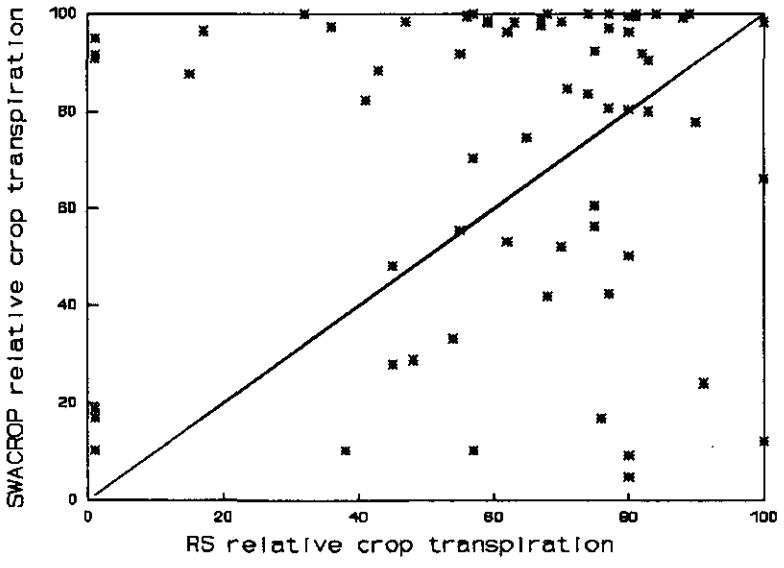


*Fig. 11 Remote sensing relative crop transpiration values against SWACROP relative crop transpiration values for all observation wells*

It is important to realize that both remote sensing and SWACROP values are not real measurements and therefore neither one of them can be seen as "true value". This makes the explanation of the differences rather complicated. Deviations can be caused by the remote sensing processing, but also by the SWACROP simulations. Another difficulty is caused by the location of the observation wells. Often the observation wells were situated at the border of a field. As it is shown in Figure 12 the borders of a field often show great variation in transpiration values. Not only the borders of the fields, but also complete fields sometimes show very irregular transpiration patterns (see Figure 12). It is obvious that comparing only one location is a rather small base, but despite these objections a detailed comparison offers possibilities to study the cause of deviations between the two methods.

Locations with great deviations were studied more precisely. False colour photographs were very useful for this study. Especially for the crop maize drought stress patterns can be detected easily on these photographs offering the possibility to validate the remote sensing values. On the false colour photographs all maize plots showed (more or less severe) drought stress patterns. Remote sensing transpiration values were low though SWACROP values indicated near optimal transpiration. Based on these observations it can be concluded that for the crop maize the remote sensing method seems to describe relative crop transpiration better than SWACROP simulations do. For the crops beets potatoes and cereals a combination of a small number of locations (respectively 11, 1 and 3) and a great variation in the deviation between both methods prevented the detection of certain trends.

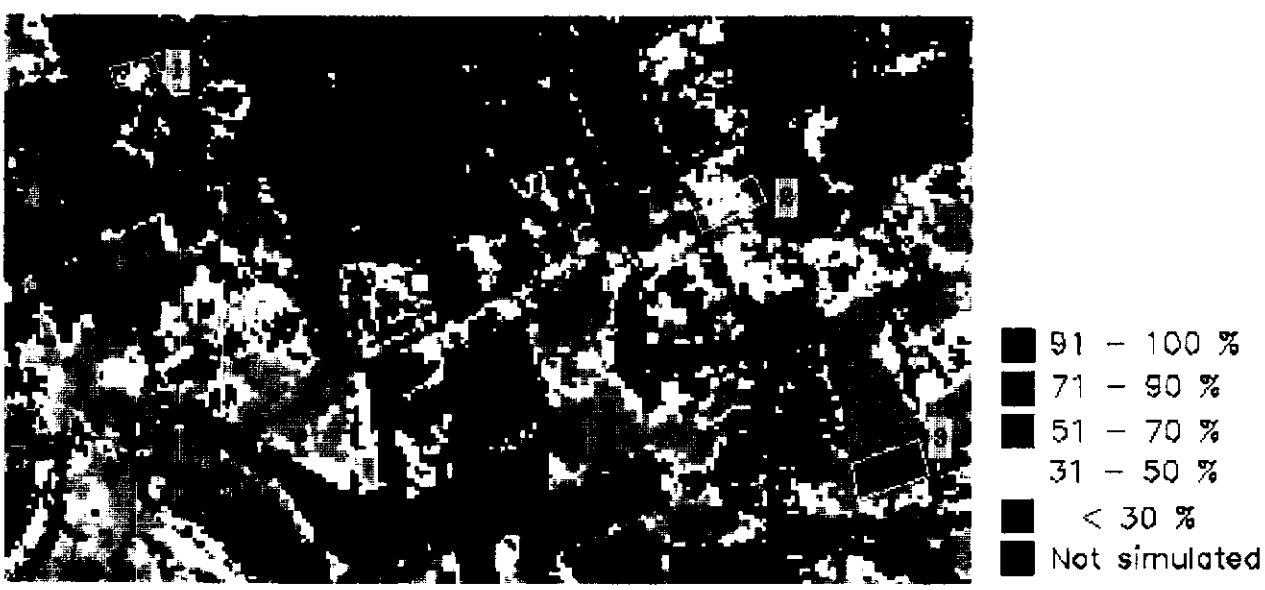


*Fig. 12 Examples of regular and irregular transpiring fields. Field 1 shows transpiration values in the whole range from 0-100%. Field 2 also shows great variation in transpiration values. Field 3 transpires almost homogeneously*

For grass the false colour photographs cannot be used to detect drought stress patterns, although they do have another application. Recently mowed grass fields cannot be used for the remote sensing method because the temperatures measured at these fields (and the transpiration values derived from those temperatures) are too much affected by the relatively warm soil. On false colour photographs these too bare fields can be detected easily. Since mowing (and also pasturing) occurs on very different times for the different plots, the length of the crop varies significantly. The length of the crop affects the measured temperature. Since the translation from crop temperature into crop transpiration occurs with mean crop values the transpiration values might be less precise. This is something that has to be kept in mind. When comparing transpiration classes this is of course of less importance than at a comparison of absolute values.

A statistical analyses was performed to study the significance of tendencies that were found and to get insight in the deviations between the SWACROP and remote sensing results. Multiple regression techniques were used to find out which variables influence the differences between remote sensing and SWACROP relative crop transpiration values. The variables used in the regression were: "soil type", "crop", "groundwater level" and "time".

In total 48.9% of the differences between remote sensing and SWACROP relative crop transpiration values can be explained with the regression variables. Compared to the 79.3% that could be explained in the large scale comparison (De Zeeuw, 1991), this is much less. This result indicates that with the improvement of the input parameters a "noise" factor becomes more important.

To study the importance of the individual variables in the explanation of the differences between remote sensing and SWACROP a step wise regression was performed. In such a regression, the variables are added step by step. Regression starts with the variable that explains most of the differences, then the second most important variable is added, then the third is added, etc. The step wise regression indicated "soil type" as the most important variable, followed by "crop" , "groundwater level" and "time" (in order of diminishing importance). Time did not significantly support in the explanation.

In the large scale comparison, drainage class and crop were the most important variables in explaining the deviations between SWACROP and remote sensing. So the results of the step wise regression confirm the improvement of the input variables groundwater level and crop. Especially drainage class (groundwater level) improved a lot, it was the most important variable in the large scale comparison, only third in the detailed comparison. This result also explains the 48.9% against the 79.3% explanation in the large scale comparison. The variable drainage class was that much important that it explained a great part of the deviations. Once improved, the influence of other variables, but also "noise" becomes more important.

Additionally the existence of interactions between the different variables was studied. An interaction seems to exist between soil type and crop, but the small amount of measurements does not allow more concrete statements about this probable interaction. This interaction might be in the SWACROP input factor "depth of the effective root zone, since the depth of the effective root zone" depends on soil type and crop. In Table 10 an overview is given of the results of the applied regression. Only the most important variables: soil type and crop are pointed out in this table. Table 11 shows the number of measurements on which the values in Table 10 are based.

*Table 10 Mean difference (%) between remote sensing and SWACROP relative crop transpiration values (RS-SWACROP) for the different simulated crops and soil types*

| Crop | Soil type | | | | | | | |
|---|---|---|---|---|---|---|---|---|
| | 1* | 4* | 6 | 8 | 9 | 13 | 16 | 22 |
| Grass | 73 | - 2 | | -40 | -16 | | -32 | |
| Beets | 12 | 5 | | 22 | 34 | -73 | | 67 |
| Potatoes | 88 | | | | | | | 1 |
| Cereals | 22 | -26 | | | | | | |
| Maize | | -67 | -91 | | -32 | | | |

*** The soiltype numbers correspond with the soil type numbers described in Annex 2**

*Table 11 Number of measurements for each combination of soil type and crop*

| Crop | Soil type | | | | | | | |
|---|---|---|---|---|---|---|---|---|
| | 1* | 4* | 6 | 8 | 9 | 13 | 16 | 22 |
| Grass | 2 | 6 | | 1 | 26 | | 12 | |
| Beets | 4 | 2 | | 2 | 1 | 1 | | 1 |
| Potatoes | 1 | 0 | | | | | | 1 |
| Cereals | 2 | 1 | | | | | | |
| Maize | | 3 | 1 | | 1 | | | |

*** The soiltype numbers correspond with the soil type numbers described in Annex 2**

As it is shown in Table 11 a lot of the differences are only based on one result. Normally these values were neglected in the interpretation of the results. An exception was made when the values were part of an overall phenomena i.e. for maize. It is obvious that for the purpose of detecting trends the number of results was actually too small. But despite the small amount of results, a few tendencies can be detected from the regression.

For the crop maize SWACROP relative crop transpiration values were always higher than the remote sensing values. Combining this with the results of a more precise study based on false colour photographs it is most likely that SWACROP overestimates the relative crop transpiration. Since this occurs at all soil types, this might imply that the input parameters for the crop maize need improvement. Of course should be stated that this conclusion was based on very few locations (5).

For soil type Hn21 (a sandy soil, Annex 2) the mean difference between remote sensing and SWACROP is always positive: so SWACROP values are lower here than remote sensing values. Because this is true for all crops (except maize) the underestimation might be caused by an underestimation of the soil hydraulic parameters of the soil. This agrees with the conclusion of De Zeeuw and Van Middelaar (1991) that on sandy soils SWACROP underestimates crop transpiration. For grass on soil type Hn21 (sandy soil) the SWACROP results are lower than the remote sensing values, for grass on soil types 9 and 16, SWACROP values are higher. This indicates an interaction between crop and soil type. As mentioned above this interaction might be in the depth of the effective root zone.

Studying the individual situation does not answer the question of what causes the deviation between SWACROP and remote sensing satisfactory. Actually the differences between the two methods (SWACROP and remote sensing) are mainly caused by differences in temporal and spatial scale. Therefore a continuing study should not result in an attempt to optimize the parameters on individual locations.

# 5 HYDROGICAL MAPPING EXPERIMENT APPLYING REMOTE SENSING

This experiment concerns a study to evaluate the importance of visual interpretation of remote sensing images in the composition of a seepage infiltration map (composed by the Province of Drenthe). In this chapter the composition of the map as performed by the provincial authorities will be explained. A description will be given of the use of the remote sensing images in verifying this map and finally the results of this experiment will be discussed.

## 5.1 Composition of the seepage infiltration map Drenthe (1 : 100,000)

The composition of the seepage infiltration map has been a rather complicated process. Annex 7 shows a part of the map as it was composed in 1989. The materials used to compose the map are shown in Table 12

***Table 12 Materials used to compose the seepage infiltration map Drenthe (1 : 100,000)***

| Material | Scale |
|---|---|
| **Studies with the hydrological model Wamil-MODFW** | **1 : 50,000** |
| **Maps of the groundwater table classes** | **1 : 50,000** |
| **Inventories of the existing canals** | **1 : 250,000** |
| **Maps of canals** | |
| **Studies with the model SBB-Femsat** | **1 : 50,000** |
| **Vegetation type maps (1 : 100,000)** | **1 : 100,000** |
| **Topographic maps (1:50.000)1 : 50,000** | **1 : 50,000** |

In four parts of the province, simulations were performed with the model MODFW (MacDonald and Harbaugh, 1984). MODFW is a quasi three dimensional steady state groundwater flow model. To simulate groundwater flow the study area was divided into a finite element network of rectangular elements. In this study each element covered 500 * 500 m, and the input (and output) information was assumed to be a mean value for that particular element. A number of horizontal layers was defined intermittently aquifers and aquitards. Horizontal flow was assumed in aquifers and vertical flow in aquitards. Infiltration (or seepage) was defined as the flux from the first to the second model layer; infiltration when the flux was positive, seepage when the flux was negative (Technische werkgroep uitwerking grondwaterplan, 1989). The second model layer consists of loam or clay ("river clay of brook loam") and varies in depth from 1 to 4 m below the surface. The simulations resulted in a calculated seepage/infiltration map. This map has been refined with the groundwater table class map. Additionally the other materials were used. Combination of all these data resulted in the distinction of three area types: Infiltration areas, seepage areas

and intermediate areas.

*Infiltration areas*
In the infiltration areas the effective precipitation infiltrates completely to the deep soil layers. These areas are generally characterized by a reduced drainage system or by the absence of a drainage system. Groundwater table classes in these areas vary usually from V to VIII.

*Seepage areas*
Groundwater that infiltrated elsewhere exfiltrates in these areas. Normally drainage systems are dense and groundwater table classes vary from II to III. In the parts of the province where MODFW calculations were performed, the seepage was quantified. In those parts the following seepage classes were distinguished: 0-1.0 $mm.d^{-1}$, 1.0-2.5 $mm.d^{-1}$, and > 2.5 $mm.d^{-1}$.

*Intermediate areas*
In these areas, part of the effective precipitation infiltrates to the deeper soil layers. The rest is discharged by the drainage system. Actually these areas are net infiltration areas with a local seepage component. Also some of the managed polders were classified as intermediate area. Parts of the Veenkoloniën, where a great variation in infiltration and seepage areas occurred, were classified as intermediate areas too (the model discretisation was too rough to take these short distance differences into account). In several intermediate areas probably seepage occurs in part of the year.

The discretisation as applied in the model MODFW has several disadvantages. Besides the inability to account for short distance differences the discretisation might cause the suppression of line formed elements. In sloping areas the mean input value may lead to both over or underestimation of the calculated flux through the model layers.

In those parts of the province where no simulations were performed, the seepage was not quantified. In these areas the reliability of the map is much smaller than in the simulated parts.

## 5.2 Use of remote sensing images

Remote sensing images are "reflections" of processes that occur at the soil surface. This must be taken into account when using remote sensing images to verify the seepage/infiltration map. For example in case of relative crop transpiration images, only the water available for the vegetation is "measured".

The northern part of map number 12 Oost was used to validate the seepage/infiltration map. This is one of the areas where MODFW simulations were performed. The remote sensing data used in this verification consisted of false

colour photographs and relative crop transpiration images. First a comparison of the relative crop transpiration images and the seepage/infiltration map was performed. In seepage areas crops were assumed to show near optimal transpiration whereas in infiltration areas a decreased transpiration was expected. For some areas that did not match these assumptions further research was started. These areas were detected on false colour photographs. The false colour photographs provided information about water access in spring: a possible indication for the occurrence of seepage. Furthermore, drought stress patterns could be detected, offering the possibility to check the relative crop transpiration images.

The MODFW input and output information was studied and combined with the other materials used in the composition of the map. Finally some areas were checked in the field. During this field survey the following points were studied: topography, density of the drainage pattern, the presence or absence of water in the ditches and the presence of specific indications of seepage for instance special vegetation and signs of perch on the borders of the ditches. Combination of all the information about the areas lead to a decision about the classification of these areas.

## 5.3 Results and discussion

In Annex 8 part of the seepage/infiltration map used for this study is presented. An overlay of this map was projected on the combined relative crop transpiration map. The resulting image is shown in Figure 13. In general this image confirms the assumption that in seepage areas crops are not expected to show strongly reduced transpiration whereas in infiltration areas reduced transpiration is more likely to occur than near optimal transpiration values. For example the Hondsrug, characterized as infiltration area, shows a lot of fields with reduced transpiration values. In the Hunze valley (seepage area) the general transpiration values are near optimal. But there are also areas that do not agree with the assumptions mentioned above. In Figure 13 some of these areas are indicated with arrows. These areas will be discussed.

### *Area 1*

Area 1, the region among the village Annen covers the area with the two rather strange indentations in the infiltration area of the Hondsrug that were classified as seepage areas. Also the area in front of the lower indentation classified as seepage area but with strongly decreased transpiration values is counted to the Annen region. Since the seepage/infiltration map is a rather generalized map the indentations seem to indicate the presence of very specific conditions. Hence these patterns were expected to show very clearly on the seepage/infiltration map. On Figure 14 it can be seen that the transpiration image does not confirm the existence of the two indentations convincingly. The false colour photograph did not confirm the strange pattern either.

To determine the origin of the classification of the two indentations the MODFW

output values were studied. In Annex 9 the MODFW output values are presented, combined with an overlay of the seepage/infiltration map. Annex 9 shows that MODFW did not simulate any seepage for the two indentations. Annex 10 shows the combined soil-groundwater table class map, again with an overlay of the seepage/infiltration map. Both indentations consist mainly of soil type Hn21 (Annex 2) with a groundwater table class VII, again no strong evidence for a classification as seepage area.

To find a decisive answer about the character of the indentations a field survey was carried out. This field survey did not confirm the existence of the strange seepage pattern either, leading to the decision to adapt the seepage/infiltration map. A proposal for a modification of the seepage infiltration map for this region is given in Figure 14. The field survey also showed an explanation for the reduced transpiration values in the area in front of the lower indentation. Normally the change from Hondsrug to Hunze valley is quite abrupt. In this specific situation the Hondsrug very gradually changes into the Hunze valley.

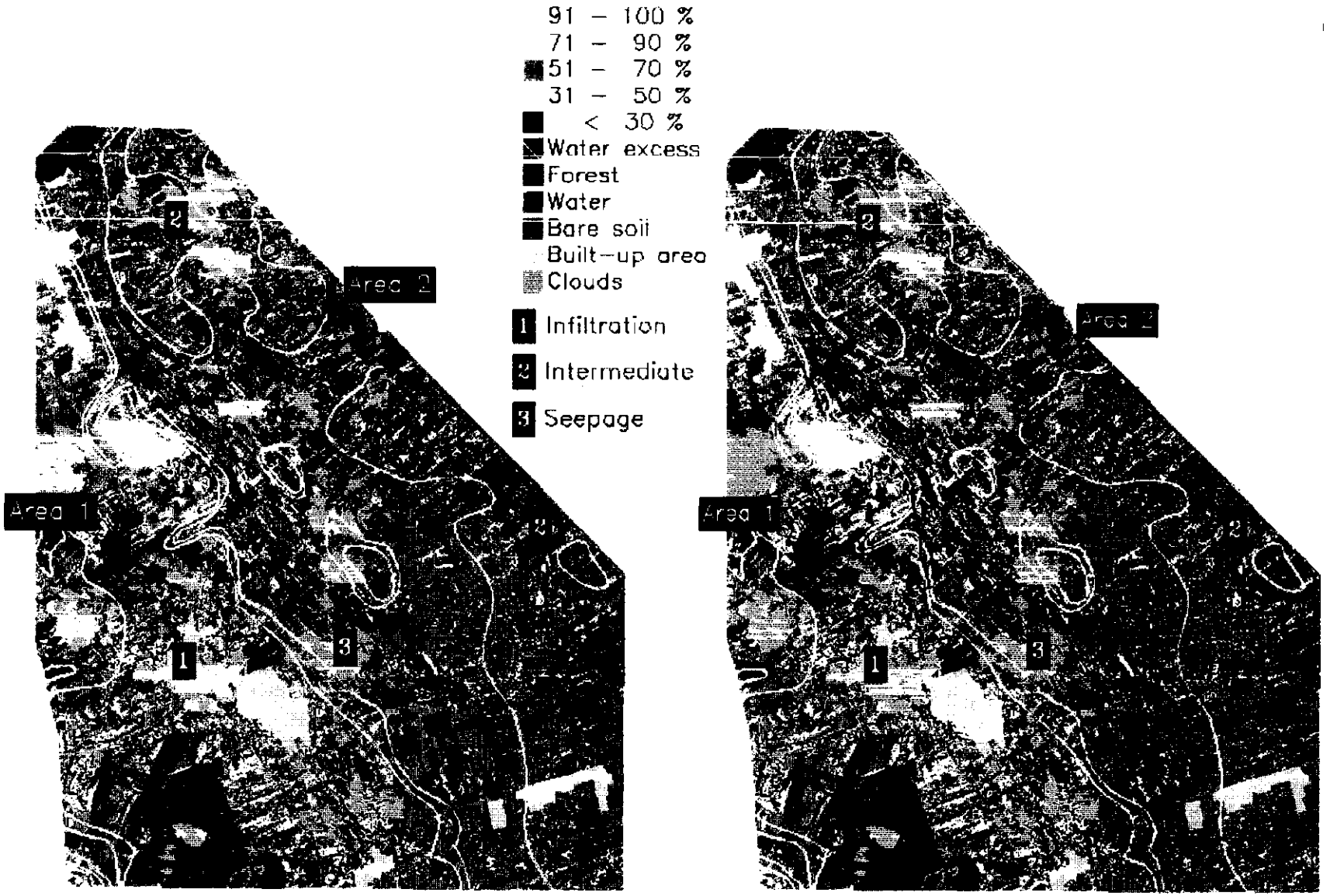


*Fig. 13 Overlay of the seepage/infiltration map on a combined relative crop transpiration image*

*Fig. 14 Proposal for some modifications in the seepage/infiltration map Drenthe*

*Area 2*

Area 2 covers a region parallel to the border of the province. From the transpiration image a zone of reduced transpiration values can be distinguished. The false colour photographs did confirm the presence of this reduced transpiration zone. On the seepage/infiltration map this zone is partly classified as intermediate area, but is cut through by a seepage area (see Figure 13).

To find the information on which the existence of such a seepage area was based the MODFW output (Annex 9) was studied. In the MODFW output part of the area was indeed simulated as seepage area, though two points, essential for the recognition of a possible intermediate zone were missing. This might be the reason that the connection between the two intermediate areas was not made. The soil map (Annex 10) does not show remarkable differences between the areas classified as intermediate and the seepage area. Hence it does not corroborate the distinction of a seepage area inbetween the intermediate zone. A field survey did not confirm the classification of the seepage/infiltration map; no indication of the existence of a seepage area was detected. Consequently also for this area a modification was needed. In Figure 14 a proposal for a modification for this situation is given. This example shows the importance of remote sensing in the recognition of regional patterns. Patterns that could not be distinguished with the material that was used originally.

As it is obvious from these examples, visual interpretation of remote sensing data (transpiration images, but also false colour photographs) can be of great help in the validation of the seepage/infiltration map. Based on this study the existing map will be validated, using the remote sensing data as indicator for strange situations. Since there is no linear relationship between crop transpiration and seepage (or infiltration) the use of remote sensing images is restricted to one of indicating. Once an area is indicated as "suspected", the specific situation has to be studied in order to be able to make a reliable decision about the classification of the area.

# 6 CONCLUSIONS AND DISCUSSION

Comparison of the variation in relative crop transpiration values according to the remote sensing approach and as simulated with SWACROP shows that SWACROP tends to simulate more extreme, either strongly diminished or near optimal, transpiration values. False colour photographs can be used to validate the remote sensing transpiration images. Especially for the crop maize false colour photographs provide a reliable check of the remote sensing results. Using these photographs it can be stated that for maize SWACROP overestimated the relative crop transpiration.

A comparison of the SWACROP and remote sensing relative crop transpiration values on individual locations shows great differences between the results of the two methods. De Zeeuw (1991) made a comparison between SWACROP and remote sensing relative crop transpiration values for different crops. The results of a comparison for different locations were disappointing. De Zeeuw indicated that especially uncertainties in the lower boundary condition caused this poor comparison. Although in this study measured ground water levels were applied no improvement of the agreement between SWACROP and remote sensing results was found.

To study the importance of the different variables a statistical analyses was performed. It was indicated that 48.9% of the deviations between SWACROP and remote sensing could be explained with the variables "soil type", "crop", "ground water level" and "time". This means that 51.1% of the deviations cannot be explained with these variables and should therefore be subscribed to "noise". With a less detailed input (De Zeeuw, 1991) 79.3% of the deviations between SWACROP and remote sensing could be explained. This indicates that with the improvement of input parameters, the factor "noise" becomes more important. "Soil type" was indicated as the most important variable in the explanation of the deviations between SWACROP and remote sensing, followed by "crop", "ground water level" and "time" respectively. Between "soil-type" and "crop" and interaction seems to exist (the number of locations prevents stronger statements). This interaction can be explained with the depth of the effective root zone, an input factor for the SWACROP simulations, which depends on crop type and soil type.

Studying the individual situation does not explain the deviation between SWACROP and remote sensing satisfactory. It is expected that the differences between the two methods are mainly caused by differences in temporal and spatial scale. Therefore a continuing study should not result in an attempt to optimize the parameters on individual locations. More attention should be paid to the sensitivity of the SWACROP model for small changes in time. Also the schematisation of the soil profile in different layers should be taken into account. Moreover the variability in the soil hydraulic functions that are assigned to the different soil

layers is of great importance. A suggestion to describe the variability in soil hydraulic functions of soils is scaling. Although this technique still underestimates the existing variability (Wösten, 1989) it may provide an impression of the accuracy of the SWACROP simulation results.

Visual interpretation of remote sensing images offers promising opportunities to detect regional patterns that cannot be distinguished with conventional methods. Furthermore it can be used to detect areas that do not match certain assumptions on transpiration. Since there is no linear relationship between crop transpiration and seepage (or infiltration) (De Zeeuw and Van Middelaar, 1991) the use of remote sensing images should be restricted to one of indicating these areas. To describe the specific hydrological situation of such areas additional research is required.

Integration of remote sensing images in the conventional composition of the seepage/infiltration map of the Province of Drenthe has lead to the reclassification of some areas. Based on the results obtained in this experiment the seepage/infiltration map will be validated using remote sensing images to indicate strange situations.

It is important to realize that once a map as the seepage/infiltration map exists it will be used as being the truth. Doubts that might exist for the constructors of the map do not exist for the users of the map. This indicates the importance of a solid check of the map, for example by visually interpreting remote sensing images.

REFERENCES


BANNINK, H.M. AND G.H. STOFFELSEN, 1984. *Bodemfysisch onderzoek ten behoeve van het tussen-10-plan.* Wageningen. STIBOKA rapport nr. 1805.

BELMANS, C., J.G. WESSELING and R.A. FEDDES, 1983. "Simulation model of the water balance of a cropped soil: SWATRE". *Journal of Hydrology,* 63:271-286.

BIJKERK, A.J., 1992. *Hydrologisch onderzoek Gasselternijveen met behulp van remote sensing en hydrologische modellen.* Wageningen, D-Staring Centrum. Rapport 191.

BLACK, T.A., W.R. GARDNER and G.W. THURTELL, 1969. "The prediction of evaporation drainage and soil water storage for a bare soil". *Soil Science,* Soc. Am. Proc., 33.

DE BAKKER, H. and J. SCHELLING, 1989. *Systeem van bodemclassificatie voor Nederland, de hogere niveaus* (with 30 pages summary: A system of soil classification for the Netherlands, The higher levels). Wageningen. Centre for Agricultural Publishing and Documentation.

DE BAKKER, H., 1979. *Major soils and soil regions in the Netherlands.* Wageningen. Centre for Agricultural publishing and Documentation.

DE ZEEUW, K. and H. VAN MIDDELAAR, 1991. "Integrated use of remote sensing and hydrological modelling to assist in the hydrological description of Drenthe, The Netherlands". In: J. HARTS, H.F.L. OTTENS & H.J. SCHOLTEN (eds), *EGIS '92;* proceedings. Utrecht, EGIS found., 1991. Vol. 2, pp 1261-1270.

FEDDES R.A., 1987. "Crop factors in relation to Makkink reference crop evapotranspiration". Comm. Hydrol. Research TNO, The Hague. Proceedings and information 39: 33-45

FEDDES, R.A., P.J. KOWALIK and H. ZARADNY, 1978. *Simulation of field water use and crop yield.* Wageningen. Centre for Agricultural Publishing and documentation,

JACKSON, R.D., R.J. REGINATO and S.B. IDSO, 1977. "Wheat canopy temperature: a practical tool for evaluating water requirements". *Water Resour. Res.* 13: 651-656.

LILLESAND, T.M. and R.W. KIEFER, 1987. *Remote Sensing and image interpretation.* New York. John Wiley & Sons,

MACDONALD, M.G. and A.W. HARBAUGH, 1984. *A modular three-dimensional finite-difference groundwater flow model.* Reston. U.S. Geological Survey.

MAKKEN, H. and F. DE VRIES, 1989. *Bodem en grondwater opnieuw in kaart, revisie van de bodemkaart van Nederland 1 : 50 000, blad 12 Oost en 17 Oost.* Wageningen, Staring Centrum. Rapport 36.

MAKKINK, G.F., 1957. "Testing the Penman formula by means of lysimeters". *Journ. Int. of Water Eng.* 11:277-288.

NIEUWENHUIS, G.J.A., E.H. SMIDT and H.A.M. THUNNISSEN, 1985. "Estimation of regional evapotranspiration of arable crops from thermal infrared images". *Int. J. Remote Sensing,* vol 6, no. 8: 1319-1334.

SOER, G.J.R., 1980. "Estimation of regional evapotranspiration and soil moisture conditions using remotely sensed crop surface temperatures". *Remote sensing of Environment* 9: 27-45.

TECHNISCHE WERKGROEP UITWERKING GRONDWATERPLAN, 1989. *Tussen-rapportage Onderzoek naar een aantal bestaande winningen, Grondwaterwinning.* Hoogeveen: 23-28.

THUNNISSEN, H.A.M. and G.J.A. NIEUWENHUIS, 1989. "An application of remote sensing and soil water balance simulation models to determine the effect of groundwater extraction on crop evapotranspiration". *Agric. Water Manag.,* 15 : 315-332.

WERKGROEP CULTUURTECHNISCH VADEMECUM, 1988. *Cultuurtechnisch vademecum.* Cultuurtechnische vereniging: 178-180.

WESSELING, J.G., 1991. *Meerjarige simulatie van grondwaterstroming voor verschillende bodemprofielen, grondwatertrappen en gewassen met het model Swatre.* Wageningen, D-Staring Centrum. Rapport 152.

WÖSTEN, J.H.M., 1989. "Use of scaling techniques to quantify variability in hydraulic functions of soils in The Netherlands". In press: Proceedings of the International Workshop on *"Field-scale water and solute flux in soils".* Monte Verità, Switzerland.

NON PUBLISHED REFERENCES

DE ZEEUW, K., in prep. *Toepassing van het hydrologisch model SWACROP en remote sensing voor de kaartbladen 12 Oost en 17 Oost.* Wageningen, D-Staring Centrum

SOER, G.J.R., 1977. *The TERGRA model: a mathematical model for the simulation of the daily behaviour of crop surface temperature and actual evapotranspiration.* Wageningen, ICW nota 1014.

THUNNISSEN, H.A.M., 1984. *Remote Sensing project Oost-Gelderland, deelrapport 4; Toepassing van hydrologische modellen en remote sensing.* Wageningen, ICW nota 1542.

VAN DER SCHANS, D.A., M.DE GRAAF and A.J. HELLINGS, 1984. *De relatie tussen wateraanvoer, verdamping en produktie, bij het gewas aardappelen.* Wageningen, ICW Nota 1539, PAGV verslag nr. 4.

ANNEX 1 CROP TYPE CLASSIFICATION SOIL MAP FOR MAP NUMBERS 12 OOST AND 17 Oost

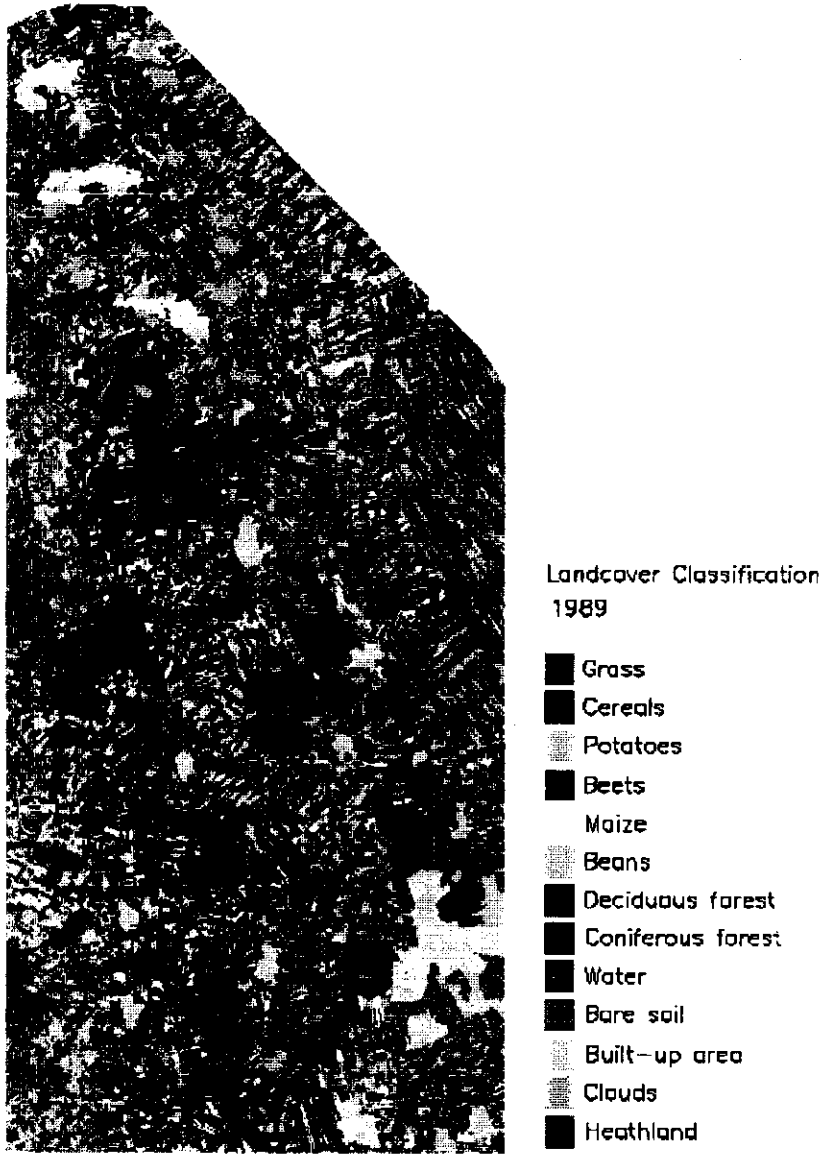


*Fig. 15 Crop type classification for the growing season of 1989 for map numbers 12 Oost and 17 Oost (De Zeeuw, 1991)*

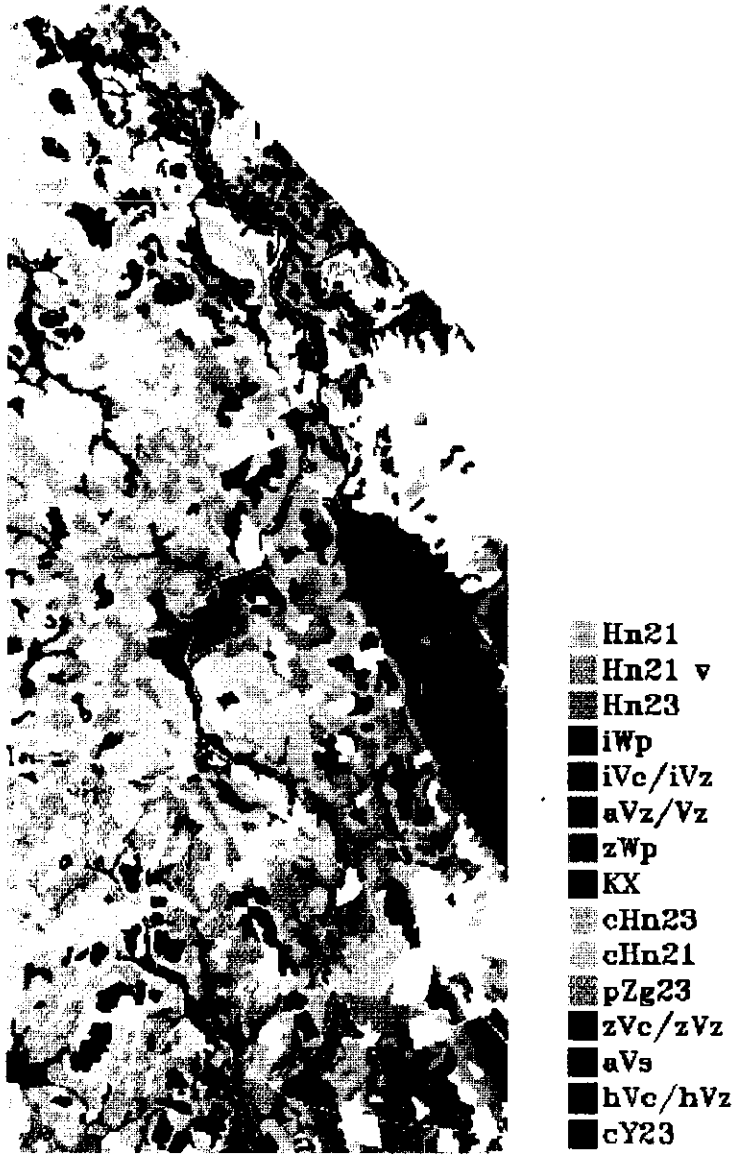


*Fig. 16 Generalized soil map for map numbers 12 Oost and 17 Oost*

## ANNEX 2 GBAL DESCRIPTION OF THE MAIN SOIL GROUPS ON MAP NUMBERS 12 OOST AND 17 OOST

The descriptions are obtained from De Bakker (1979) and De Bakker and schelling (1989)

| | | |
|---|---|---|
| 1 | Hn21 | Gleyic podzol. Topsoil loamy fine sand. Shallow A1 horizon (0-15 cm). |
| 2 | Hn21v | Gleyic podzol. topsoil disturbed |
| 4 | Hn23 | Gleyic podzol. Topsoil very loamy fine sand. Shallow A1 horizon (0-15 cm) |
| 6 | iWp | Humose sand overlying a thin remnant over cut-over peat, overlying a buried Podzol in Pleistocene sand, viz. cover sand. |
| 8 | iVz/iVz | Distric Histosol. Soil of the cut-over raised bogs district. |
| 9 | aVz/Vz | Eutric Histosol |
| 13 | cHn23 | Gleyic podzol. Topsoil very loamy fine sand. Medium thick A1 horizon (30-50 cm) |
| 15 | cHn21 | Gleyic podzol. Topsoil loamy fine sand. Medium thick A1 horizon (30-50 cm) |
| 16 | Zg23 | Humic gley soil. Topsoil (very) loamy fine sand. p; pleistocene. |
| 18 | zVc/zVz | Distric Histosol. Typic sandy top layer. Soil of the cut-over raised bog district. |
| 19 | zVc/zZv | Eutric Histosol. Sandy topsoil. |
| 20 | aVs | Distric Histosol |
| 22 | cY23 | Leptic podzol. medium thick (30-50 cm) A1 consisting of loamy fine sand. |

ANNEX 3 OVERVIEW OF MAIN SOIL GROUPS, THICKNESS OF THE LAYERS THEY CONSIST OF AND THE EFFECTIVE ROOT ZONE FOR POTATOES, BEETS, GRASS, CEREALS AND MAIZE

**Table 13 Main soil groups, thickness of the layers they consist of and the effective root zone for potatoes and beets (Bannink and Stoffelsen, 1984)**

| Soil type | | Eff. root zone | | Subsoil | | | | | | | |
|---|---|---|---|---|---|---|---|---|---|---|---|
| no. | code | depth (cm - mv.) | unit number | first layer | | second layer | | third layer | | fourth layer | |
| | | | | depth (cm - mv.) | unit | depth (cm - mv.) | unit | depth (cm - mv.) | unit | depth (cm - mv.) | unit |
| 1 | Hn21 | 0-30 | 2 | > 30 | 13a | | | | | | |
| 2 | Hn21→ | 0-35 | 2 | > 35 | 13a | | | | | | |
| 3 | Hn21x | 0-30 | 2 | 30- 80 | 15 | > 80 | 16 | | | | |
| 4 | Hn23 | 0-30 | 4 | 30- 50 | 15 | > 50 | 14 | | | | |
| 5 | Hn23x | 0-30 | 4 | 30- 50 | 15 | 50- 80 | 14 | > 80 | 16 | | |
| 6 | iWp | 0-40 | 7 | 40- 60 | 17 | > 60 | 13a | | | | |
| 7 | iWpx | 0-40 | 7 | 40- 50 | 17 | 50-100 | 13a | >100 | 16 | | |
| 8 | iVc/iVz | 0-25 | 8 | 25- 40 | 17 | 40-120 | 19 | >120 | 22 | | |
| 9 | aVz/Vz | 0-25 | 9 | 25- 80 | 20 | > 80 | 22 | | | | |
| 10 | zWp | 0-35 | 10 | 35- 50 | 18 | > 50 | 13a | | | | |
| 11 | zWpx | 0-35 | 10 | 25- 50 | 21 | 50- 90 | 14 | > 90 | 16 | | |
| 12 | KX | 0-20 | 5 | 20- 35 | 14 | > 35 | 16 | | | | |
| 13 | cHn23 | 0-50 | 4 | 50- 60 | 15 | > 60 | 14 | | | | |
| 14 | cHn21 | 0-50 | 4 | 50- 60 | 15 | 60- 80 | 14 | > 80 | 16 | | |
| 15 | cHn21 | 0-45 | 3 | > 45 | 13a | | | | | | |
| 16 | pZg23 | 0-40 | 1 | > 40 | 22 | | | | | | |
| 17 | pZg23x | 0-35 | 1 | 35- 80 | 22 | > 80 | 16 | | | | |
| 18 | zVc/zVz[1] | 0-25 | 10 | 25- 50 | 17 | 50-100 | 18 | 100 | 22 | | |
| 19 | zVc/zVz[2] | 0-30 | 10 | 30-100 | 20 | >100 | 22 | | | | |
| 20 | aVs | 0-20 | 11 | 20-120 | 18 | >120 | 13a | | | | |
| 21 | hVc/hVz | 0-20 | 12 | 20-100 | 20 | >100 | 22 | | | | |
| 22 | cY23 | 0-50 | 6 | 50- 70 | 23 | > 70 | 24 | | | | |

[1] inside the cut-over raised bog district
[2] outside the cut-over raised bog district

Table 14 Main soil groups, thickness of the layers they consist of and the effective root zone for grass (Thunnissen, 1984 and Bijkerk, 1992)

| Soil type | | Eff. root zone | | Subsoil | | | | | | | |
|---|---|---|---|---|---|---|---|---|---|---|---|
| no. | code | depth (cm - mv.) | unit number | first layer | | second layer | | third layer | | fourth layer | |
| | | | | depth (cm - mv.) | unit | depth (cm - mv.) | unit | depth (cm - mv.) | unit | depth (cm - mv.) | unit |
| 1 | Hn21 | 0-20 | 2 | > 20 | 13a | | | | | | |
| 2 | Hn21→ | 0-25 | 2 | > 25 | 13a | | | | | | |
| 3 | Hn21x | 0-20 | 2 | 20- 80 | 15 | > 80 | 16 | | | | |
| 4 | Hn23 | 0-20 | 4 | 20- 50 | 15 | > 50 | 14 | | | | |
| 5 | Hn23x | 0-20 | 4 | 20- 50 | 15 | 50- 80 | 14 | > 80 | 16 | | |
| 6 | iWp | 0-25 | 7 | 25- 60 | 17 | > 60 | 13a | | | | |
| 7 | iWpx | 0-25 | 7 | 25- 50 | 17 | 50-100 | 13a | >100 | 16 | | |
| 8 | iVc/iVz | 0-20 | 8 | 20- 40 | 17 | 40-120 | 19 | >120 | 22 | | |
| 9 | aVz/Vz | 0-20 | 9 | 20- 80 | 20 | > 80 | 22 | | | | |
| 10 | zWp | 0-25 | 10 | 25- 50 | 18 | > 50 | 13a | | | | |
| 11 | zWpx | 0-25 | 10 | 25- 50 | 21 | 50- 90 | 14 | > 90 | 16 | | |
| 12 | KX | 0-15 | 5 | 15- 35 | 14 | > 35 | 16 | | | | |
| 13 | cHn23 | 0-30 | 4 | 30- 40 | 4 | 40- 60 | 15 | > 60 | 14 | >80 | 16 |
| 14 | cHn21 | 0-30 | 4 | 30- 40 | 4 | 40- 80 | 15 | 60- 80 | 14 | | |
| 15 | cHn21 | 0-30 | 3 | 30- 40 | 3 | > 40 | 13a | | | | |
| 16 | pZg23 | 0-30 | 1 | > 30 | 22 | | | | | | |
| 17 | pZg23x | 0-25 | 1 | 25- 80 | 22 | >100 | 22 | | | | |
| 18 | zVc/zVz[1] | 0-20 | 10 | 20- 50 | 17 | 50-100 | 18 | 100 | 22 | | |
| 19 | zVc/zVz[2] | 0-25 | 10 | 25-100 | 20 | >100 | 22 | | | | |
| 20 | aVs | 0-15 | 11 | 15-120 | 18 | >120 | 13a | | | | |
| 21 | hVc/hVz | 0-20 | 12 | 20-100 | 20 | >100 | 22 | | | | |
| 22 | cY23 | 0-30 | 6 | 30- 50 | 6 | 50- 70 | 23 | > 70 | 24 | | |

[1] inside the cut-over raised bog district
[2] outside the cut-over raised bog district

Table 15 Main soil groups, thickness of the layers they consist of and the effective root zone for cereals and maize (Thunnissen, 1984 and Bijkerk, 1992)

| Soil type | | Eff. root zone | | Subsoil | | | | | | | |
|---|---|---|---|---|---|---|---|---|---|---|---|
| no. | code | depth (cm - mv.) | unit number | first layer | | second layer | | third layer | | fourth layer | |
| | | | | depth (cm - mv.) | unit | depth (cm - mv.) | unit | depth (cm - mv.) | unit | depth (cm - mv.) | unit |
| 1 | Hn21 | 0-40 | 2 | > 40 | 13a | | | | | | |
| 2 | Hn21→ | 0-45 | 2 | > 45 | 13a | | | | | | |
| 3 | Hn21x | 0-40 | 2 | 40- 80 | 15 | > 80 | 16 | | | | |
| 4 | Hn23 | 0-40 | 4 | 40- 50 | 15 | > 50 | 14 | | | | |
| 5 | Hn23x | 0-40 | 4 | 40- 50 | 15 | 50- 80 | 14 | > 80 | 16 | | |
| 6 | iWp | 0-55 | 7 | 55- 65 | 17 | > 65 | 13a | | | | |
| 7 | iWpx | 0-55 | 7 | 55- 60 | 17 | 60-100 | 13a | >100 | 16 | | |
| 8 | iVc/iVz | 0-35 | 8 | 35- 45 | 17 | 45-120 | 19 | >120 | 22 | | |
| 9 | aVz/Vz | 0-35 | 9 | 35- 80 | 20 | > 80 | 22 | | | | |
| 10 | zWp | 0-50 | 10 | 50- 65 | 18 | > 65 | 13a | | | | |
| 11 | zWpx | 0-50 | 10 | 50- 65 | 21 | 65- 90 | 14 | > 90 | 16 | | |
| 12 | KX | 0-20 | 5 | 20- 35 | 14 | > 35 | 16 | | | | |
| 13 | cHn23 | 0-70 | 4 (tot 50 cm) | 50- 60 | 15 | > 60 | 14 | | | | |
| 14 | cHn21 | 0-70 | 4 (tot 50 cm) | 50- 60 | 15 | 60- 80 | 14 | > 80 | 14 | | |
| 15 | cHn21 | 0-65 | 3 (tot 45 cm) | > 45 | 13a | | | | | | |
| 16 | pZg23 | 0-50 | 1 | > 50 | 22 | | | | | | |
| 17 | pZg23x | 0-45 | 1 | 45- 80 | 22 | > 80 | 16 | | | | |
| 18 | zVc/zVz[1] | 0-30 | 10 | 30- 50 | 17 | 50-100 | 18 | 100 | 22 | | |
| 19 | zVc/zVz[2] | 0-35 | 10 | 35-100 | 20 | >100 | 22 | | | | |
| 20 | aVs | 0-20 | 11 | 20-120 | 18 | >120 | 13a | | | | |
| 21 | hVc/hVz | 0-20 | 12 | 20-100 | 20 | >100 | 22 | | | | |
| 22 | cY23 | 0-75 | 6 (tot 60 cm) | 60- 80 | 23 | > 80 | 24 | | | | |

[1] inside the cut-over raised bog district
[2] outside the cut-over raised bog district

ANNEX 4 DESCRIPTION OF A SWACROP INPUT FILE

Table 16 Example of a Swacrop input file (GRAS103.INP).
Before running Swacrop all input files need to be renamed to SWADAT.INP

| | |
|---|---|
| AA | GRAS103.INP, Hn23 , GRASS, f mak, mod SWACROP |
| AB | 0 2 5 0 2 1 1 0 0 1 |
| AC | GRAS103.OUT |
| AE | GRAS103.SOL |
| AF | 0 0 0 0 1 |
| AH | 60. 273. 0.2 0.005 |
| | 10 5 0.005 |
| BA | 0 0 0.02 0.0 |
| | 0.0 365. 366. |
| | -10. -25. -25. -200. -800. -500. -8000. |
| BG | 6.3877 -17.7030 16.0697 |
| BH | 0 |
| | 1 |
| BI | 60 20.0 273 20.0/ |
| | 1 |
| BJ | 60 1.0 273 1.0/ |
| | 1 |
| BL | 60 1.0 222 1.0 232 0.9 273 0.9/ |
| CA | 400. 3 40 4 10 40 |
| CB | 5. 5. 5. 5. 5. 5. 5. 5. 5. 5. |
| | 5. 5. 5. 5. 5. 5. 5. 5. 5. 5. |
| | 10. 10. 10. 10. 10. 10. 10. 10. 10. 10. |
| | 20. 20. 20. 20. 20. 20. 20. 20. 20. 20. |
| CC | [VERHEIJDEN.SWACROP.BS]B4.DAT |
| | [VERHEIJDEN.SWACROP.BS]O15.DAT |
| | [VERHEIJDEN.SWACROP.BS]O14.DAT |
| CD | 0.0 |
| | 3 |
| CF | 60 58.5 73 42.0 104 53.0 137 100.0/ |
| | 166 117.0 199 136.0 227 151.0/ |
| | 257 157.0 273 156.5/ |
| CM | [VERHEIJDEN.SWACROP.meteo]eext.met |
| CN | 0.54 -4.0 |

GENERAL INPUT DATA

AA Header containing the name of the input file, soil type and crop
AB Choosing type of initial and boundary conditions, type of output to check computing stage, crop production, irrigation and compartment size.
- Ground water level is input at the bottom of the soil profile.
- Potential evapotranspiration ($cm.d^{-1}$) is calculated with the Makkink equation.

AC Filename of the output file containing the water balance.
- Name output file : GRAS103.OUT.

AE Filename of the output file containing soil-profile data.
- Name soil-output file : GRAS103.SOL.

AF Choice of the output written to the output file containing the soil profile data.
- Only volume of water extracted by roots is written to GRAS103.SOL.

AG Describes the calculation period and size of time step.
- Simulation starts JD (Julian Day number) 60 and ends JD 273.
- Maximum value of a time step allowed is 0.2 d.
- Maximum change of soil moisture content is 0.005 $cm^3.cm^{-3}$.

AH Describes the limits for the pressure head iteration process.
- Maximum number of iterations allowed during a time step is 10.
- Maximum number of decrements of the time step when the iteration criterion is not reached is 5.
- Iteration criterion is 0.005.

CROP INPUT DATA

BA Description of the Sink term and root extraction pattern.
- Sink term according to Feddes.
- Linear relationship between the points Hlim3 and Hlim4.

BG Describes the Leaf Area Input - Soil Cover function.
BH Describes the precipitation interception function.
- Standard function is used.

BI Describes the rooting depth (daynr - rooting depth).
BJ Describes the soil cover (daynr - soil cover).
BL Describes the crop factor (daynr - crop factor).

SOIL INFUT DATA

CA Describes the geometry of the soil profile:
- depth of the soil profile is 400 cm;
- 3 different types of soil layers;
- 40 compartments;
- bottom compartment of first layer is compartment 4;
- bottom compartment of second layer is compartment 10;
- bottom compartment of third layer is compartment 40.

CB Describes the thickness of all compartments in the soil profile (cm).

CC Files containing the soil physical parameters of the defined layers.

CD Maximum thickness of ponding layer on the soil surface.

CF Groundwater levels (daynr - groundwater level). SWACROP performs linear interpolation between the given days.

CM File that describes the boundary conditions at the top of the profile.

CN Description of transformation coefficients for changing global radiation to net radiation and vice versa.

## ANNEX 5 OVERVIEW OF THE EXISTING GROUNDWATER TABLE CLASSES (GT'S)

On soil maps the groundwater level (reference is field level) is indicated. To do this a national system of groundwater table classes was developed. This system is based on the mean highest (GHG) and mean lowest (GLG). These quantities indicate the level to which, under average circumstances, the groundwater raises in winter and drops in summer. For the soil maps 1 : 50,.000 seven classes exist, additionally four drier varieties can be distinguished.

***Table 17** Classification of the groundwater table classes (Werkgroep Cultuurtechnisch vademecum, 1988)*

| | Gt | | | | | | |
|---|---|---|---|---|---|---|---|
| | I | II[1] | III[1] | IV | V[1] | VI | VII[2] |
| **GHG in cm below field level** | (<20) | (<40) | <40 | <40 | >40 | 40-80 | >80 |
| **GLG in cm below field level** | <50 | 50-80 | 80-120 | >120 | >120 | >120 | (>160) |

[1] **A* behind these Gt's means a drier part; GHG is deeper that 25 cm below field level**
[2] **A* behind these Gt's means a very dry part; GHG deeper than 140 cm below field level**

ANNEX 6 OVERVIEW OF ALL SIMULATION RESULTS

Table 18 Overview of soil type, remote sensing relative crop transpiration, SWACROP simulation result, groundwater level and map number for all observation wells on June 20

| Nr. | Crop type | Soil type* | Remote sensing level | SWACROP | Ground-water number | Julian day | Map number |
|---|---|---|---|---|---|---|---|
| 4 | grass | 9 | 80.00 | 80.45 | 115.80 | 171 | 12 oost |
| 6 | grass | 9 | 83.00 | 80.07 | 137.70 | 171 | 12 oost |
| 7 | wheats | 1 | 76.00 | 16.77 | 155.30 | 171 | 12 oost |
| 17 | wheats | 4 | 74.00 | 100.00 | 121.70 | 171 | 17 oost |
| 24 | grass | 9 | 75.00 | 92.29 | 116.40 | 171 | 12 oost |
| 25 | grass | 9 | 82.00 | 91.92 | 129.00 | 171 | 12 oost |
| 27 | wheats | 1 | 1.00 | 16.93 | 145.10 | 171 | 12 oost |
| 38 | grass | 9 | 1.00 | 90.79 | 113.40 | 171 | 17 oost |
| 41 | grass | 9 | 57.00 | 70.49 | 163.00 | 171 | 17 oost |
| 42 | grass | 9 | 88.00 | 99.25 | 67.70 | 171 | 17 oost |
| 45 | grass | 16 | 17.00 | 96.43 | 134.90 | 171 | 17 oost |
| 48 | grass1 | 6 | 47.00 | 98.50 | 112.40 | 171 | 17 oost |
| 49 | grass | 16 | 56.00 | 99.62 | 82.40 | 171 | 17 oost |
| 51 | grass | 9 | 75.00 | 60.71 | 189.60 | 171 | 17 oost |
| 64 | grass | 1 | 80.00 | 9.21 | 156.60 | 171 | 17 oost |
| 76 | grass | 9 | 81.00 | 99.62 | 61.30 | 171 | 17 oost |
| 80 | grass | 4 | 83.00 | 90.60 | 161.40 | 171 | 17 oost |
| 82 | grass | 9 | 70.00 | 98.50 | 74.20 | 171 | 17 oost |
| 85 | grass | 16 | 63.00 | 98.31 | 116.20 | 171 | 17 oost |
| 92 | grass | 16 | 100.00 | 98.31 | 225.10 | 171 | 17 oost |
| 99 | grass | 9 | 74.00 | 83.65 | 127.00 | 171 | 17 oost |
| 104 | grass | 9 | 77.00 | 97.18 | 91.40 | 171 | 17 oost |
| 107 | grass | 4 | 90.00 | 77.82 | 175.10 | 171 | 17 oost |
| 110 | grass | 16 | 62.00 | 96.24 | 131.80 | 171 | 17 oost |
| 111 | grass | 9 | 67.00 | 98.87 | 72.00 | 171 | 17 oost |
| 117 | grass | 16 | 67.00 | 97.56 | 124.00 | 171 | 17 oost |
| 119 | grass | 4 | 80.00 | 96.24 | 135.40 | 171 | 17 oost |
| 128 | grass | 8 | 59.00 | 98.50 | 93.50 | 171 | 17 oost |
| 134 | grass | 9 | 59.00 | 98.12 | 81.70 | 171 | 17 oost |

* 1: Hn21, 2: Hn21v, 4: Hn23, 6: iWp, 8: iVz/iVz, 9: aVz/Vz, 13: cHn23, 15: cHn21, 16: Zg23, 18: zVc/zVz, 19: zVc/zZv, 20: aVs, 22: cY23.
A short description of the soil types is given in ANNEX1

Table 19 Overview of soil type, remote sensing relative crop transpiration, SWACROP simulation result, groundwater level and map number for all observation wells on August 23

| Nr. | Crop type | Soil type* | Remote sensing level | SWACROP | Ground-water number | Julian day | Map number |
|---|---|---|---|---|---|---|---|
| 4 | grass | 9 | 70.00 | 52.20 | 118.20 | 235 | 12 oost |
| 5 | potatoes | 22 | 45.00 | 28.00 | 323.50 | 235 | 17 oost |
| 6 | grass | 9 | 77.00 | 42.37 | 150.00 | 235 | 12 oost |
| 8 | potatoes | 1 | 100.00 | 12.00 | 128.90 | 235 | 12 oost |
| 12 | beets | 1 | 1.00 | 18.70 | 132.40 | 235 | 12 oost |
| 13 | beets | 8 | 68.00 | 41.93 | 201.70 | 235 | 17 oost |
| 18 | beets | 8 | 75.00 | 56.37 | 147.60 | 235 | 12 oost |
| 24 | grass | 9 | 55.00 | 55.59 | 118.60 | 235 | 12 oost |
| 25 | grass | 9 | 45.00 | 48.14 | 130.60 | 235 | 12 oost |
| 33 | grass | 4 | 48.00 | 28.81 | 250.60 | 235 | 17 oost |
| 34 | maize | 9 | 68.00 | 100.00 | 99.30 | 235 | 12 oost |
| 36 | beets | 9 | 100.00 | 66.29 | 117.10 | 235 | 12 oost |
| 42 | grass | 9 | 32.00 | 100.00 | 69.70 | 235 | 17 oost |
| 45 | grass | 16 | 65.00 | 74.58 | 156.60 | 235 | 17 oost |
| 48 | grass | 16 | 77.00 | 100.00 | 124.10 | 235 | 17 oost |
| 49 | grass | 16 | 57.00 | 100.00 | 48.10 | 235 | 17 oost |
| 51 | grass | 9 | 54.00 | 33.22 | 215.00 | 235 | 17 oost |
| 53 | maize | 4 | 36.00 | 97.29 | 233.20 | 235 | 17 oost |
| 54 | maize | 4 | 43.00 | 88.48 | 355.60 | 235 | 17 oost |
| 64 | grass | 1 | 80.00 | 4.75 | 194.60 | 235 | 17 oost |
| 74 | beets | 1 | 38.00 | 10.20 | 279.30 | 235 | 17 oost |
| 76 | grass | 9 | 89.00 | 100.00 | 81.50 | 235 | 17 oost |
| 78 | beets | 4 | 80.00 | 50.43 | 231.31 | 235 | 17 oost |
| 79 | grass | 9 | 81.00 | 100.00 | 93.10 | 235 | 17 oost |
| 80 | grass | 4 | 77.00 | 80.68 | 187.50 | 235 | 17 oost |
| 82 | grass | 9 | 84.00 | 100.00 | 72.50 | 235 | 17 oost |
| 86 | beets | 1 | 81.00 | 10.20 | 212.80 | 235 | 17 oost |
| 87 | beets | 4 | 80.00 | 99.43 | 140.30 | 235 | 17 oost |
| 90 | grass | 13 | 15.00 | 87.54 | 259.10 | 235 | 17 oost |
| 96 | beets | 1 | 57.00 | 10.20 | 329.30 | 235 | 17 oost |
| 101 | beets | 22 | 91.00 | 24.08 | 370.50 | 235 | 17 oost |
| 104 | grass | 9 | 55.00 | 91.86 | 104.70 | 235 | 17 oost |
| 110 | grass | 16 | 41.00 | 82.37 | 151.00 | 235 | 17 oost |
| 111 | grass | 9 | 81.00 | 100.00 | 83.10 | 235 | 17 oost |
| 113 | grass | 4 | 71.00 | 84.75 | 180.80 | 235 | 17 oost |
| 115 | grass | 16 | 62.00 | 53.22 | 147.10 | 235 | 17 oost |
| 121 | maize | 6 | 1.00 | 91.53 | 308.60 | 235 | 17 oost |
| 134 | grass | 9 | 59.00 | 98.64 | 103.60 | 235 | 17 oost |
| 137 | maize | 4 | 1.00 | 94.92 | 295.30 | 235 | 17 oost |

ANNEX 7 PART OF THE SEEPAGE INFILTRATION MAP DRENTHE (1989)

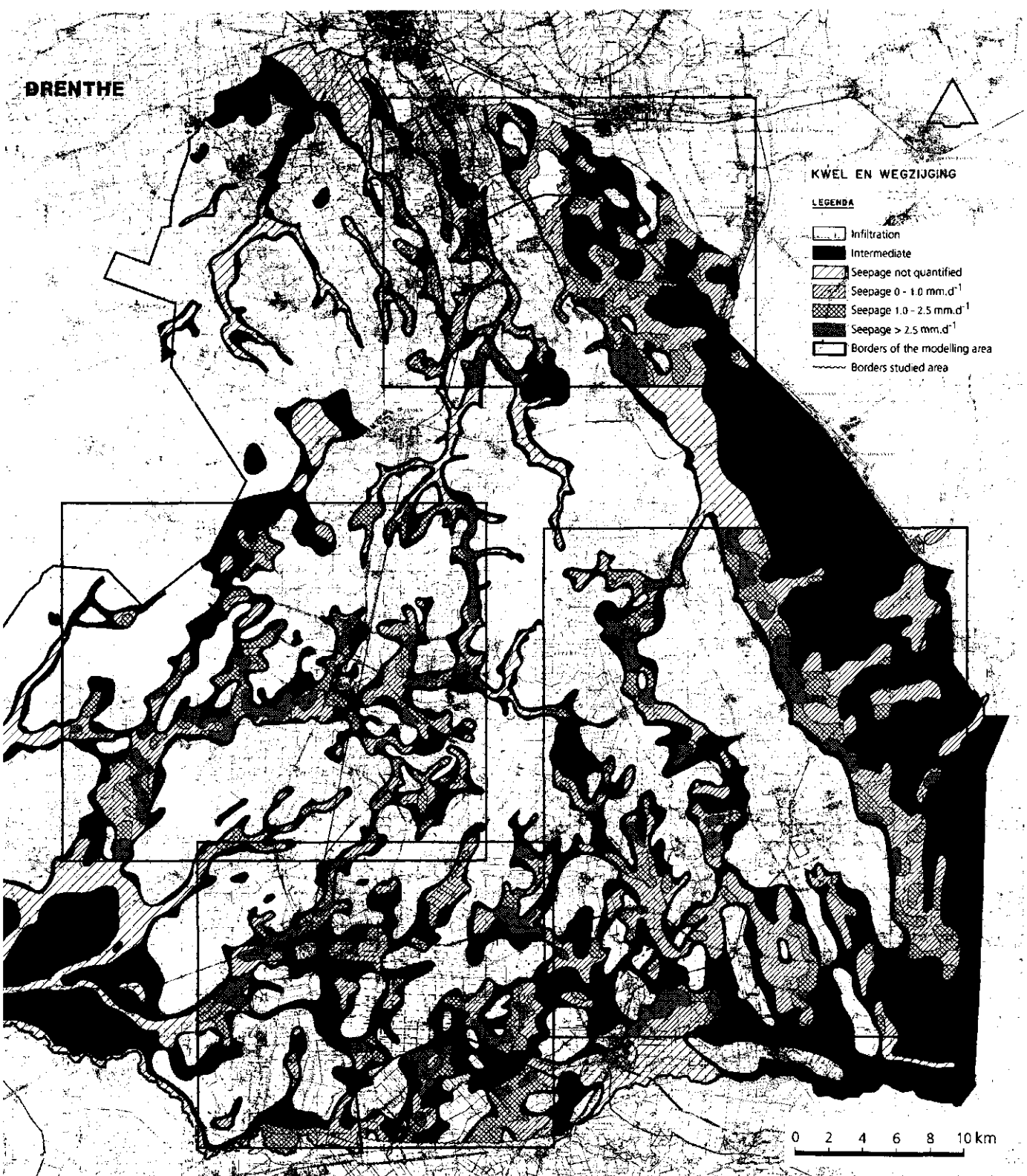


*Fig. 17 Part of the seepage/infiltration map Drenthe (1989)*

# ANNEX 8 SEEPAGE/INFILTRATION MAP FOR THE NORTHERN PART OF MAP NUMBER 12 OOST

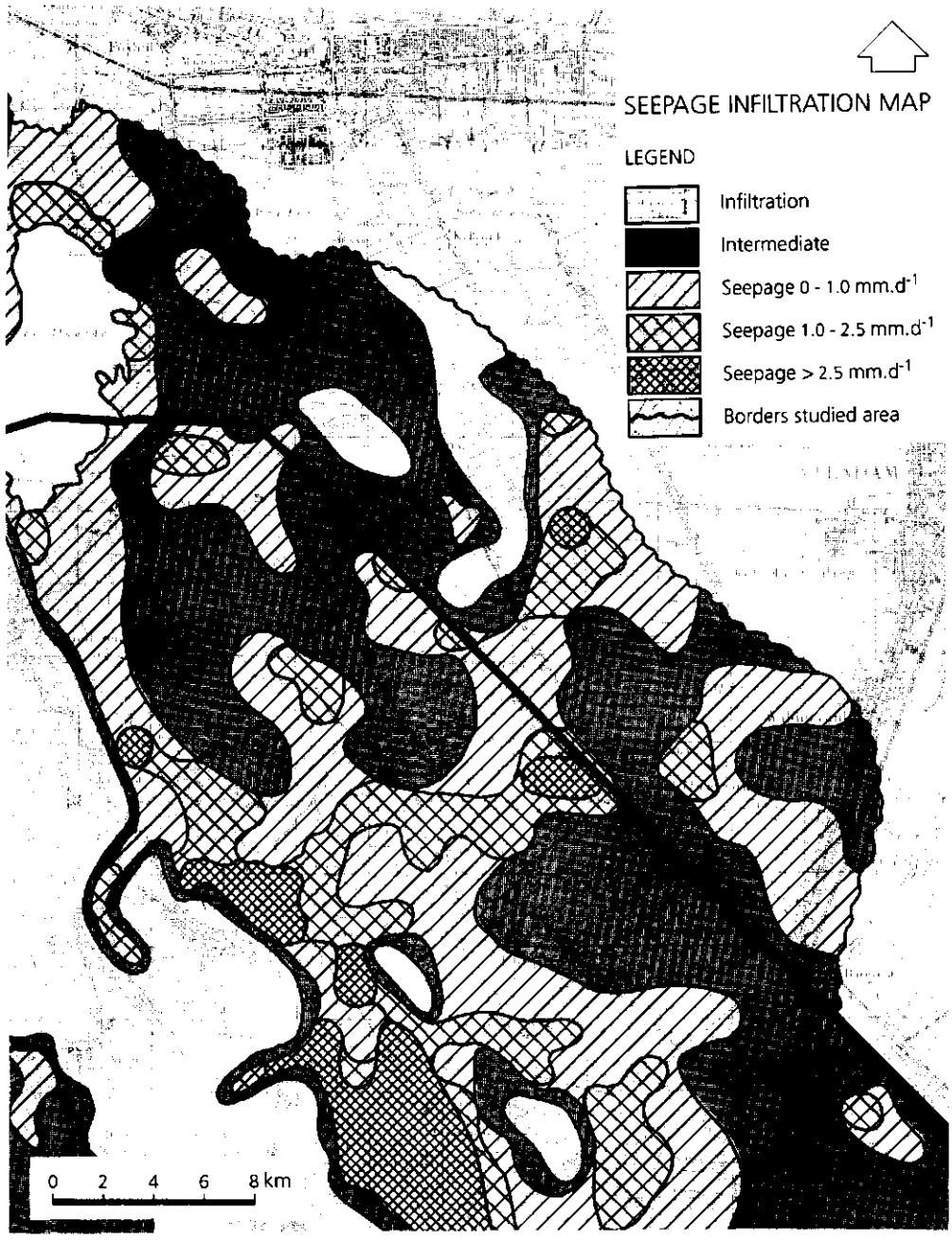


*Fig. 18 Seepage/infiltration map for the Northern part of map number 12 Oost*

ANNEX 9 MODFW OUTPUT VALUES COMBINED WITH AN OVERLAY OF THE SEEPAGE/INFILTRATION MAP

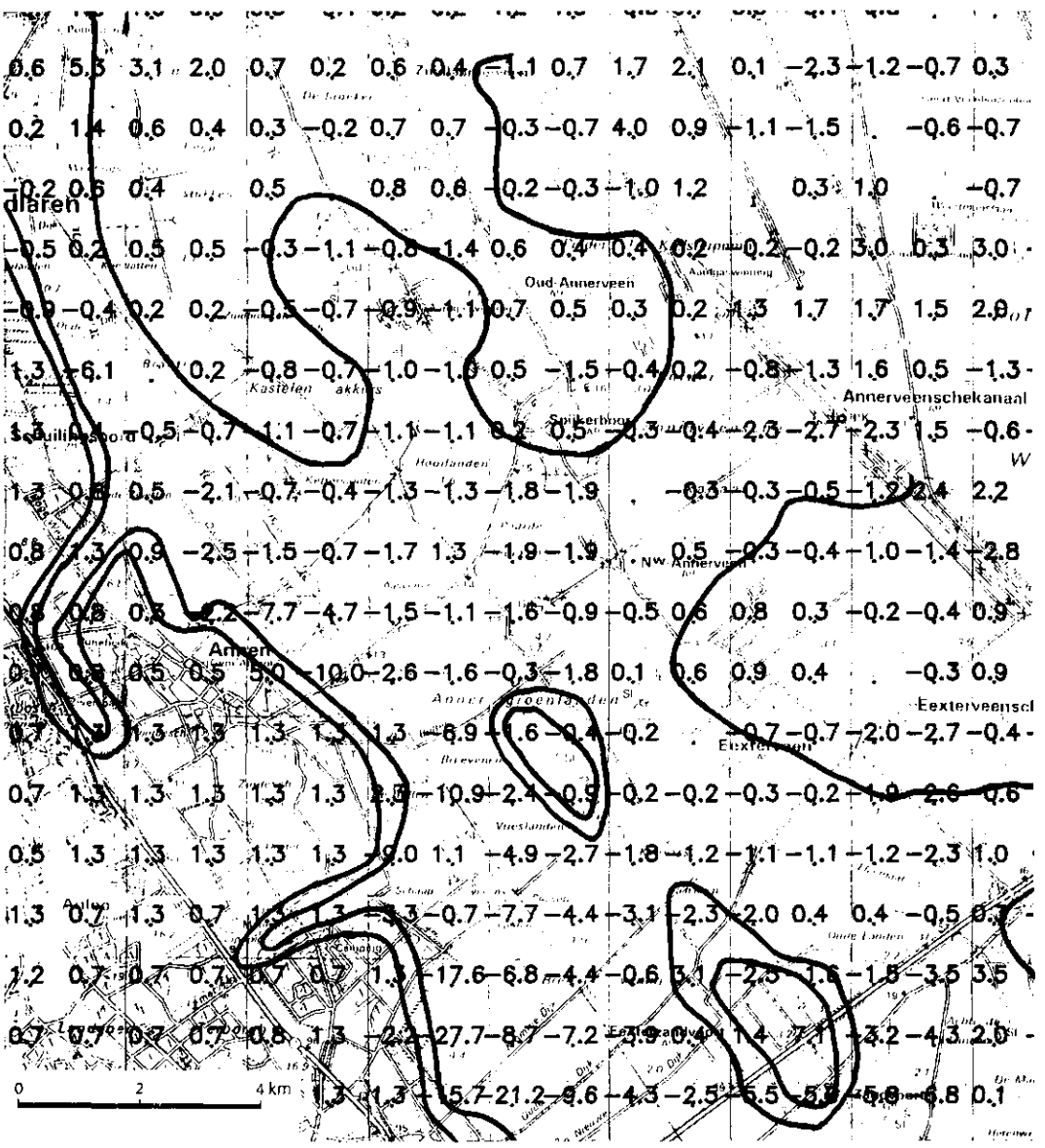


*Fig. 19 Flux from first to second model layer (mm/day) as calculated with the model MODFW combined with an overlay of the seepage/infiltration map (northern part of map number 12 Oost).*

ANNEX 10 SOIL MAP COMBINED WITH AN OVERLAY OF THE SEEPAGE INFILTRATION MAP

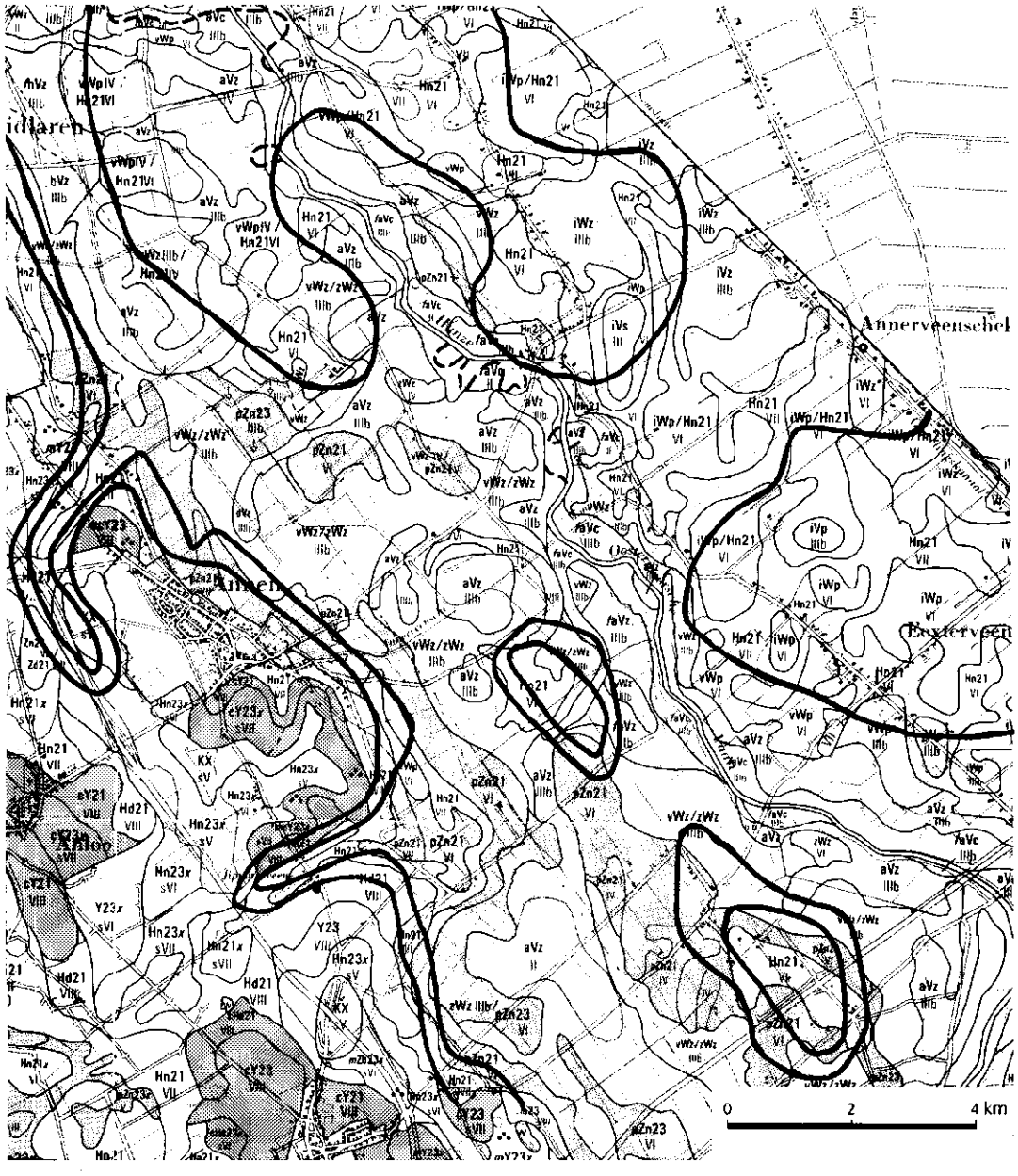


*Fig. 20 Soil-water table class map (Makken and De Vries, 1989) with an overlay of the seepage/infiltration map (northern part of map number 12 Oost)*